

Robust Nonparametric Regression for Compositional Data: the Simplicial–Real case

Ana M. Bianco¹, Graciela Boente¹,
Wenceslao González–Manteiga²
Francisco Gude Sampedro² and Ana Pérez–González³

¹ Universidad de Buenos Aires and CONICET

² Universidad de Santiago de Compostela

³ Universidad de Vigo

Abstract

Statistical analysis on compositional data has gained a lot of attention due to their great potential of applications. A feature of these data is that they are multivariate vectors that lie in the simplex, that is, the components of each vector are positive and sum up a constant value. This fact poses a challenge to the analyst due to the internal dependency of the components which exhibit a spurious negative correlation. Since classical multivariate techniques are not appropriate in this scenario, it is necessary to endow the simplex of a suitable algebraic-geometrical structure, which is a starting point to develop adequate methodology and strategies to handle compositions. We centered our attention on regression problems with real responses and compositional covariates and we adopt a nonparametric approach due to the flexibility it provides. Aware of the potential damage that outliers may produce, we introduce a robust estimator in the framework of nonparametric regression for compositional data. The performance of the estimators is investigated by means of a numerical study where different contamination schemes are simulated. Through a real data analysis the advantages of using a robust procedure is illustrated.

1 Introduction

In practice in many circumstances data sets are compositional in the sense that only the proportions between variables are informative. This frequently occurs in official statistics, chemical and geological sciences and economic applications, just to mention some disciplines with potential interest on this issue. Typical examples of compositional data include the composition of a rock is expressed in terms of the proportion or percentage of different compounds, household expenses are expressed as percentages of the monthly budget, nutrient information on food labels, proportions of pollutants in air. [Pawlowsky-Glahn and Buccianti \(2011\)](#) and the references therein constitute a guide on compositional data. This type data is usually represented by proportions or percentages.

Loosely speaking, compositional data refers to a multivariate vector with non-negative components that sum up a constant, typically the unity. A key point is that in this kind of data the information that matters lies in the relation between the compositional elements. That is, the interest of one component relies on its relative size with respect to others.

Formally speaking, a compositional datum is a D -vector $\mathbf{x} = (x_1, \dots, x_D)^\top$ belonging to the simplex

$$\mathcal{S}^D = \left\{ \mathbf{x} = (x_1, \dots, x_D) : x_i \geq 0, 1 \leq i \leq D, \sum_{i=1}^D x_i = \kappa \right\}, \quad (1)$$

where κ is a positive constant. This is the simplicial sample space. Since the information is given in terms of the ratio between the components, it is preserved by multiplying by any positive number, thus typically κ is taken equal to 1. The particular geometry of the simplex deserves the development of specific methodology to analyze compositional data where the focus is on the relative information, not on the absolute one. Regression models, variable selection, classification, clusters and dimensionality reduction techniques are necessary in this context. In this paper, we focus on regression when the response is scalar and the covariates are compositional.

The compositional data have been studied from two points of view. The Raw Data Analysis (RDA) that uses multivariate methods to standardized raw data, we can mention among the articles that follow this approach [Baxter et al. \(2005\)](#) and [Baxter and Freestone \(2006\)](#). However, the constraint to a constant sum may be a serious restriction for the application of standard statistical techniques since spurious negative correlation is present among the components of the composition, see [Pearson \(1897\)](#). In this sense, in compositional analysis, data lie in a non-Euclidean space that must be equipped with a suitable structure and geometry. [Aitchison \(1982\)](#) and the first edition of [Aitchison \(2003\)](#) that appeared in 1986 stated the basis of a geometry for the simplex that settled down a pioneer proposal that gave the simplex the structure of a vector space, known as Aitchison geometry. In this way he overcame the problem of a constraint sum and from there, a toolbox with different statistical methods was developed by tailoring to the context of compositional data very popular techniques such as regression, cluster, classification and discriminant analysis, among others.

In the last years some reviews of compositional data have been published showing the great interest that this area has received, let us mention [Aitchison \(2003\)](#), [Alenazi \(2021\)](#), [Van den Boogaart et al. \(2020\)](#) and [Greenacre \(2021\)](#).

Regression techniques play a central role in statistical analysis and we focus on the case where we deal with compositional covariates and real scale responses. Historically, the first approach that appeared in this setting was the parametric one through linear models. [Aitchison and Bacon-Shone \(1984\)](#) in a seminal paper proposed removing the constant-sum constraint by transforming the compositions using log-contrast models based on transformations of the compositional data. It is worth noticing that in this setting the direct interpretation of linear models is not as direct as with regular covariates. [Di Marzio et al. \(2015\)](#) addressed the nonparametric perspective which provides flexible techniques and introduced nonparametric estimators of the regression function by means of simplicial kernels. However, since these kernel estimators are based on weighted means they are susceptible to the influence of outliers among the responses what motivates our robust proposals.

In our contribution we first overview the basic geometrical notions related to the simplex, the natural sample space of compositional data. Unlike the regular case, the basic operations of sum and scalar multiplication are not close in this domain, so it is a necessary step to endow the simplex an algebraic-geometrical structure to get an Euclidean vector space. Secondly, we review the main probabilistic models on the simplex.

We then focus on our purpose which is to provide robust estimators for the nonparametric regression model with real response and compositional regressors.

The organization of the manuscript is as follows. In [Section 2](#) we introduce Aitchison geometry and three isomorphisms that transform the simplex in the real space. We also briefly outline probabilistic models on the simplex as well. In [Section 3](#) we recall the definition of simplicial kernels, we overview the nonparametric approach followed by [Di Marzio et al. \(2015\)](#) and just after, we introduce our two robust proposals. Furthermore, in this section we also describe a bandwidth selection method with the purpose of being resistant to outliers. Finally, in [Section 4](#) we report the results of a numerical experiment that was carried out in order to compare, under different models and contamination schemes, the performance of our robust estimators with their classical counterparts based on least squares. [Section 5](#) illustrates the advantages of using a robust procedure on a real data set.

2 Basic concepts

Henceforth, we will assume that $\kappa = 1$ in (1), i.e., \mathcal{S}^D refers to

$$\mathcal{S}^D = \left\{ \mathbf{x} = (x_1, \dots, x_D) : x_i \geq 0, 1 \leq i \leq D, \sum_{i=1}^D x_i = 1 \right\}.$$

2.1 Key geometrical notions in the simplex

It is well known that when a random element, such as a vector or a variable, is constrained to take values in a space $\chi \subset \mathbb{R}^D$, ordinary operations such as addition or multiplication by a scalar may lead to non compatible results, in the sense that the new element may lie outside χ . For, instance, the real line with the classical sum and multiplication by scalars is a vector space and the ordinary inner product and Euclidean distance preserve compatibility with them. However, this geometrical structure is not adequate for the positive real line, see [Mateu-Figueras and Pawlowsky-Glahn \(2008\)](#) for an illustrative description of these problems. This elementary example shows that when dealing with a constrained domain it is necessary to embed the sample space in a suitable geometrical structure.

Aitchison geometry gives the simplex the structure of a real vector space. It adapts the fundamental notions of translation, scaling, inner product and orthogonal projection that we know in the classical geometry to this particular framework. Perturbation and powering are the basic operations that play the role of addition (or translation) and scaling, respectively, (see [Aitchison, 1982, 2003](#)). Given $\mathbf{x}, \mathbf{y} \in \mathcal{S}^D$ and $\alpha \in \mathbb{R}$, the perturbation between them and the powering are defined, respectively, as

$$\mathbf{x} \oplus \mathbf{y} = \mathcal{C}(x_1 y_1, \dots, x_D y_D) \quad \text{and} \quad \alpha \odot \mathbf{x} = \mathcal{C}(x_1^\alpha, \dots, x_D^\alpha),$$

where for $\mathbf{u} \in \mathbb{R}^D$ such that $u_j > 0$, for all $1 \leq j \leq D$, the closure operator is

$$\mathcal{C}(\mathbf{u}) = \mathcal{C}(u_1, \dots, u_D) = \left(\frac{u_1}{\sum_{j=1}^D u_j}, \dots, \frac{u_D}{\sum_{j=1}^D u_j} \right)^\top.$$

Note that for the perturbation the neutral element is $\mathbf{n} = \mathcal{C}(1, \dots, 1) = (1/D, \dots, 1/D)^\top$ and the opposite of \mathbf{x} is $\mathcal{C}(1/x_1, 1/x_2, \dots, 1/x_D)$, while that repeated perturbation is a particular case of powering, for example, $\mathbf{x} \oplus \mathbf{x} = 2 \odot \mathbf{x}$. The simplex with these two operations becomes a vector space and (\mathcal{S}^D, \oplus) is a commutative group. Besides, the difference perturbation, which is the opposite operation of perturbation, is then defined as

$$\mathbf{x} \ominus \mathbf{y} = \mathbf{x} \oplus ((-1) \odot \mathbf{y}) = \mathcal{C} \left(\frac{x_1}{y_1}, \dots, \frac{x_D}{y_D} \right),$$

while the Aitchison inner product is given by

$$\langle \mathbf{x}, \mathbf{y} \rangle_a = \frac{1}{D} \sum_{i < j} \log \left(\frac{x_i}{x_j} \right) \log \left(\frac{y_i}{y_j} \right) = \sum_{j=1}^D \log \left(\frac{x_j}{g_D(\mathbf{x})} \right) \log \left(\frac{y_j}{g_D(\mathbf{y})} \right),$$

where $g_D(\mathbf{x}) = \left(\prod_{\ell=1}^D x_\ell \right)^{1/D}$ is the geometric mean of components of \mathbf{x} . Hence, with this set of operations the simplex gains the structure of a $D - 1$ dimensional Euclidean vector space. The Aitchison norm and distance, related to this product, are defined as

$$\|\mathbf{x}\|_a = \langle \mathbf{x}, \mathbf{x} \rangle_a = \sum_{j=1}^D \left\{ \log \left(\frac{x_j}{g_D(\mathbf{x})} \right) \right\}^2,$$

$$d_a^2(\mathbf{x}, \mathbf{y}) = \frac{1}{D} \sum_{i < j} \left\{ \log \left(\frac{x_i}{x_j} \right) - \log \left(\frac{y_i}{y_j} \right) \right\}^2 = \sum_{j=1}^D \left\{ \log \left(\frac{x_j}{g_D(\mathbf{x})} \right) - \log \left(\frac{y_j}{g_D(\mathbf{y})} \right) \right\}^2.$$

Finally, to it is easy to see that

$$d_a(\mathbf{x}, \mathbf{y}) = \|\mathbf{x} \ominus \mathbf{y}\|_a \quad \text{and} \quad \|\mathbf{x}\|_a = d_a(\mathbf{x}, \mathbf{n}).$$

It is worth mentioning that with this geometrical structure \mathcal{S}^D verifies the usual properties that relates the distance with the sum and scaling operations, thus in the simplex we have for any $\mathbf{x}, \mathbf{y}, \mathbf{z} \in \mathcal{S}^D$ and $\alpha \in \mathbb{R}$

$$d_a(\mathbf{z} \oplus \mathbf{x}, \mathbf{z} \oplus \mathbf{y}) = d_a(\mathbf{x}, \mathbf{y}) \quad \text{and} \quad d_a(\alpha \odot \mathbf{x}, \alpha \odot \mathbf{y}) = |\alpha| d_a(\mathbf{x}, \mathbf{y}).$$

A simple way to analyze compositional data relies on isomorphisms that transform from the simplex to the real space. The first transformation introduced from \mathcal{S}^D to \mathbb{R}^D , due to [Aitchison \(1982\)](#), is the additive logratio transformation (*alr*) given by

$$alr(\mathbf{x}) = \left\{ \log \left(\frac{x_1}{x_D} \right), \dots, \log \left(\frac{x_{D-1}}{x_D} \right) \right\} \quad (2)$$

The *alr* transformation is one-to one and its inverse denoted $inv.alr : \mathbb{R}^{D-1} \rightarrow \mathcal{S}^D$ is given by

$$inv.alr(\mathbf{y}) = inv.alr(y_1, \dots, y_{D-1}) = \mathcal{C} \{ \exp y_1, \dots, \exp y_{D-1}, 1 \}$$

Since *alr* transforms the simplicial space in the whole \mathbb{R}^{D-1} , transformed data may be analyze with standard multivariate statistical techniques and then inference conclusions can be transferred to the original data. However, a drawback of *alr* is that it does not preserve distances. An isometrical version is obtained using the geometric mean as divisor, resulting the centred log-ratio transformation (*clr*) which is given by $clr : \mathcal{S}^D \rightarrow \mathbb{R}^D$ and

$$clr(\mathbf{x}) = \left(\log \left(\frac{x_1}{g_D(\mathbf{x})} \right), \dots, \log \left(\frac{x_D}{g_D(\mathbf{x})} \right) \right).$$

Note that, for any $\mathbf{x} \in \mathcal{S}^D$, $clr(\mathbf{x})$ is a constrained vector of \mathbb{R}^D taking values in \mathcal{V} , where \mathcal{V} stands for the hyperplane $\mathcal{V} = \{ \mathbf{z} \in \mathbb{R}^D : \sum_{j=1}^D z_j = 0 \}$, meaning that $clr(\mathcal{S}^D) = \mathcal{V}$.

Therefore, inverse of the *clr* transformation, denoted $inv.clr$, may be defined with domain in \mathcal{V} as

$$inv.clr(\mathbf{y}) = \mathcal{C}(\exp(\mathbf{y})).$$

As noted by [Pawlowsky-Glahn et al. \(2015\)](#) *clr* transformation is symmetric in the components, but at the price of being constrained in the image sample: the trasnformed sample lies in a plane, in fact the components sum up zero, implying that the covariance matrix of $clr(\mathbf{x})$ is singular. Note that for any $\mathbf{x} \in \mathcal{S}^D$, we have that $clr(\mathbf{x}) \in \mathbb{R}^D$ is orthogonal to the vector $\mathbf{1}_D$.

[Egozcue et al. \(2003\)](#) introduced the isometric log-ratio (*ilr*) transformation of D-parts compositions. Such transformation gives coordinates in \mathbb{R}^{D-1} (*ilr*-coordinates), and has some advantages with respect to the previously proposed transformations. Let the set $(\mathbf{e}_1, \dots, \mathbf{e}_{D-1})$ be an orthonormal basis of \mathcal{S}^D and denote as \mathbf{U} the associated basis-contrast matrix, i.e., the $D \times (D-1)$ matrix with i -th column given by centered log-ratio (*clr*), $clr(\mathbf{e}_i)$, $i \in 1, \dots, D-1$. Since $\mathbf{1}_D^\top clr(\mathbf{e}_j) = 0$ and the orthonormal basis satisfies $\langle \mathbf{e}_i, \mathbf{e}_j \rangle_a = \delta_{ij}$, where δ_{ij} is the Kroenecker delta, we get that

$$\mathbf{U}^\top \mathbf{U} = \mathbf{I}_{D-1} \quad \text{and} \quad \mathbf{U} \mathbf{U}^\top = \mathbf{I}_D - \frac{1}{D} \mathbf{1}_D \mathbf{1}_D^\top,$$

where \mathbf{I}_k is the k -dimensional identity matrix and $\mathbf{1}_k$ is the k -dimensional vector with components equal to 1. The *ilr* transformation related to \mathbf{U} , lets say $ilr = ilr_{\mathbf{U}}$, where $ilr : \mathcal{S}^D \rightarrow \mathbb{R}^{D-1}$, is the one-to-one linear transformation that relates the vector $\mathbf{x}^* \in \mathbb{R}^{D-1}$ to $\mathbf{x} \in \mathcal{S}^D$, as follows

$$\mathbf{x}^* = ilr(\mathbf{x}) = \mathbf{U}^\top clr(\mathbf{x}) = \mathbf{U}^\top \log(\mathbf{x}). \quad (3)$$

Then, the inverse of the *ilr* transformation related to \mathbf{U} , denoted $inv.ilr : \mathbb{R}^{D-1} \rightarrow \mathcal{S}^D$, is defined as

$$inv.ilr(\mathbf{z}) = \mathcal{C}(\exp\{\mathbf{U}\mathbf{z}\}) ,$$

see for instance [Tsagris et al. \(2023\)](#) for further details.

From now on, $\|\cdot\|$, $\langle \cdot, \cdot \rangle$ stand for the usual Euclidean norm and inner product in \mathbb{R}^{D-1} .

As mentioned, the *ilr* transformation defines an isomorphism between \mathcal{S}^D and \mathbb{R}^{D-1} , that is, for $\mathbf{x}, \mathbf{y} \in \mathcal{S}^D$, $\alpha \in \mathbb{R}$, we have that

$$ilr(\mathbf{x} \oplus \mathbf{y}) = ilr(\mathbf{x}) + ilr(\mathbf{y}) \quad \text{and} \quad ilr(\alpha \odot \mathbf{x}) = \alpha ilr(\mathbf{x})$$

and exhibits the property of being isometric meaning that

$$d_a(\mathbf{x}, \mathbf{y}) = \|ilr(\mathbf{x}) - ilr(\mathbf{y})\| ,$$

It is also worth noticing that $\|\mathbf{x}\|_a = \|ilr(\mathbf{x})\|$. Furthermore, if $\mathbf{x}^* = ilr(\mathbf{x})$ and $\mathbf{y}^* = ilr(\mathbf{y})$, then

$$\langle \mathbf{x}, \mathbf{y} \rangle_a = \langle \mathbf{x}^*, \mathbf{y}^* \rangle = \sum_{j=1}^{D-1} x_j^* y_j^*$$

meaning that Aitchison norms and distances are translated into ordinary ones in *ilr*-space.

2.2 Probability models on the simplex

Probability models are fundamental in order to endow a behavioral pattern to a random phenomenon and they are a very useful tool in Statistics since they give a support to the statistical techniques and analysis. We will introduce the building blocks related to this topic, more details can be found, for instance, in Chapter 6 in [Pawlowsky-Glahn et al. \(2015\)](#).

We recall that a random variable \mathbf{X} is a random composition if all its possible values lie in \mathcal{S}^D , which we assumed is endowed with the Aitchison geometry (perturbation and powering operations plus Aitchison inner product, norm and distance).

So, let $\mathbf{X} = (X_1, \dots, X_D)^\top$ be a random composition with possible values in \mathcal{S}^D and for a chosen orthonormal basis of \mathcal{S}^D consider the contrast matrix \mathbf{U} . Therefore, as seen in (3) the *irl*-coordinates related to the selected basis are

$$\mathbf{X}^* = (X_1^*, \dots, X_{D-1}^*)^\top = irl(\mathbf{X}) = \mathbf{U}^\top \log(\mathbf{X}) ,$$

where \mathbf{X}^* is a random variable with sample space in the real $D - 1$ dimensional space. We will deal with continuous random variables in \mathcal{S}^* , that is given \mathbf{X} we assume that there exists a nonnegative real function $f^* : \mathbb{R}^{D-1} \rightarrow \mathbb{R}$, defined almost everywhere, such that for any Borelian set $B \subset \mathbb{R}^{D-1}$

$$\mathbb{P}(ilr(\mathbf{X}) \in B) = \int_B f^*(\mathbf{x}^*) d\mathbf{x}^* .$$

In this case, f^* is known as the probability density function of the *irl*-coordinates, while $f(\mathbf{x}) = f^*(ilr(\mathbf{x}))$, defined for any \mathbf{x} in the simplex, is the probability density function of \mathbf{X} on \mathcal{S}^D . It is worth noticing that even when the expression of f^* depends on the chosen orthonormal basis, the pdf on the simplex doen not.

Now, note that probability models are in many cases presented in terms of a probability density function (pdf) that is referred to a measure, usually the reference is the Lebesgue measure which is natural in a real space. When the simplex endowed with the Aitchison geometry is the sample space,

the natural reference measure is the Aitchison one, that introduces an alternative expression of the pdf's even when we are dealing with the same probability law. The Aitchison measure on the simplex is built from the Lebesgue measure on the *ilr*-coordinates space. In fact, let λ denote the Lebesgue measure and consider an orthonormal basis on \mathcal{S}^D , its the corresponding *ilr*-transformation into coordinates and \mathcal{B} , an open interval on \mathbb{R}^{D-1} , given by

$$\mathcal{B} = \{[x_1, \dots, x_{D-1}] \in \mathbb{R}^{D-1} \text{ such that } a_i < x_i < b_i, 1 \leq i \leq D-1\} .$$

If the corresponding *ilr*-interval on \mathcal{S}^D is \mathcal{B}^* , i.e., $\mathcal{B}^* = \text{ilr.inv}(\mathcal{B})$, the Aitchison measure of \mathcal{B}^* is $\lambda_a(\mathcal{B}^*) = \lambda(\mathcal{B})$.

In the next paragraphs, we recall the definition of two important distributions on the simplex: the Dirichlet distribution and the normal distribution on the simplex.

The Dirichlet distribution, labelled $\mathcal{D}(\boldsymbol{\alpha})$ with $\boldsymbol{\alpha} = (\alpha_1, \dots, \alpha_D)^\top$, is obtained as the closure independent gamma-distributed random variables that are equally scaled. More precisely, we say that the variable $\mathbf{X} \in \mathcal{S}^D$ has a multivariate density function of the Dirichlet distribution if

$$f(\mathbf{x}; \boldsymbol{\alpha}) = \frac{\Gamma\left(\sum_{j=1}^D \alpha_j\right)}{\prod_{j=1}^D \Gamma(\alpha_j)} \prod_{j=1}^D x_j^{\alpha_j-1} \mathbb{I}_{\{\mathbf{x} \in \mathcal{S}^D\}}, \quad (4)$$

where $\alpha_j > 0$ for $j = 1, \dots, D$ and Γ is the Gamma function. This expression of the pdf is with respect to the Lebesgue measure. It is strictly supported on the simplex and it reduces to the beta distribution when $D = 2$. The Dirichlet distribution for compositional data was proposed in [Connor and Mosimann \(1969\)](#), later on numerous publications analyze and apply this distribution, see [Hijazi and Jernigan \(2009\)](#) and [Tsagris and Stewart \(2018\)](#) and the book by [Aitchison \(2003\)](#), among others. The Dirichlet distribution can also be formulated in terms of the Aitchison measure, the corresponding representation can be found, for instance, in [Pawlowsky-Glahn et al. \(2015\)](#).

The Logistic Normal distribution was introduced by [Aitchison and Shen \(1980\)](#). The idea beneath this distribution is to assume that the *arl*-representation of the random composition follows a multivariate normal distribution. The original definition of this distribution is from the *alr*-coordinates of the compositional variates and a posterior application or change of variable theorem. Given $\boldsymbol{\mu} \in \mathbb{R}^{D-1}$ and a symmetric positive definite matrix $\boldsymbol{\Sigma} \in \mathbb{R}^{(D-1) \times (D-1)}$, the vector \mathbf{X} follows an additive logistic distribution $N_{\mathcal{S}^D}(\boldsymbol{\mu}, \boldsymbol{\Sigma})$ in the simplex space if $\text{alr}(\mathbf{x}) = \log(\mathbf{x}^{(-D)}/x_D)$ where $\mathbf{x}^{(-D)} = (x_1, \dots, x_{D-1})^\top$, follows a normal $N_{D-1}(\boldsymbol{\mu}, \boldsymbol{\Sigma})$. However, the same distribution is obtained if it is assumed that the *irl*-coordinates have a normal joint density, which is easier to handle due to the orthonormal basis that mediates in the *irl*-transformation. Thus, we say that the random composition \mathbf{X} follows a Logistic Normal distribution on the simplex if \mathbf{X}^* is normally distributed on \mathbb{R}^{D-1} , i.e. $\mathbf{X}^* \sim N_{D-1}(\boldsymbol{\mu}, \boldsymbol{\Sigma})$, with density function with respect to the Lebesgue measure in \mathbb{R}^{D-1} given by

$$f(\mathbf{x}^*) = (2\pi)^{-(D-1)/2} |\boldsymbol{\Sigma}|^{-1/2} \exp\left[-\frac{1}{2}(\mathbf{x}^* - \boldsymbol{\mu})^\top \boldsymbol{\Sigma}^{-1}(\mathbf{x}^* - \boldsymbol{\mu})\right]. \quad (5)$$

In this case, we denote $\mathbf{X} \sim N_{\mathcal{S}^D}(\boldsymbol{\mu}, \boldsymbol{\Sigma})$. Equivalently, the density function with respect to the Aitchison measure in \mathcal{S}^D is of the form

$$f(\mathbf{x}) = (2\pi)^{-(D-1)/2} |\boldsymbol{\Sigma}|^{-1/2} \exp\left[-\frac{1}{2}(\text{ilr}(\mathbf{x}) - \boldsymbol{\mu})^\top \boldsymbol{\Sigma}^{-1}(\text{ilr}(\mathbf{x}) - \boldsymbol{\mu})\right],$$

for $\mathbf{x} \in \mathcal{S}^D$. In this representation, $\boldsymbol{\mu}$ and $\boldsymbol{\Sigma}$ depend on the chosen *irl*-transformation, that is on the selected contrast matrix \mathbf{U} .

See also [Mateu-Figueras and Pawlowsky-Glahn \(2008\)](#) and [Egozcue et al. \(2012\)](#) for more details.

3 Regression model

Modeling is an important task in statistical analysis, where regression techniques play a central role. The interest focuses on the relationship between variables with the aim of prediction or either understanding the way in which a set of regressor variables (\mathbf{X}), namely the covariates, affect the behaviour of a dependent variable, i.e., the response (Y). Regression problems involving compositions deserve a particular approach due to the structure of these data. We concentrate on the case where we deal with compositional covariates and real scale response. The first to appear was the parametric treatment of the problem. However, in this setting the interpretability of models is more complex than with regular variables. As mentioned in [Greenacre \(2021\)](#), even if a linear model is postulated, the explanation of the effect of the coefficients is not as direct as with real-valued variables. In fact, the traditional interpretation that the magnitude of the impact of a change in one unit in a certain variable, remaining the others fixed, is the corresponding coefficient is no longer valid in this context, where the modification of one element of the composition necessarily alters the others due to constraint sum.

In the setting of linear models, [Scheffé \(1958\)](#) early considered the problem of prediction when dealing with mixtures of components and in [Scheffé \(1963\)](#) design of experiments is treated in the framework of compositions. [Aitchison and Bacon-Shone \(1984\)](#) considered log-contrast models based on the *alr*-transformation given in (2) to circumvent the constant sum. They proposed to study linear models of the form

$$Y = \theta_0 + \sum_{j=1}^{D-1} \theta_j \log \frac{x_j}{x_D} + \epsilon,$$

where ϵ represents the error term and they also included quadratic log-contrast versions of these models. A drawback of this approach is that variables are not treated symmetrically since the practitioner has to choose a component for the common divisor. Further advances in the Euclidean geometry of the simplex such as the introduction of the *irl*-transformation given in (3) and also on the logistic-normal distribution described above, settled down the basis of expressions of the regression model in coordinates and the use of ordinary least squares, see [Egozcue et al. \(2012\)](#) for details.

There exists a vast literature on the parametric-driven approach, [Coenders and Pawlowsky-Glahn \(2020\)](#) reviews many of the alternative parametrizations that were proposed for the simplicial-real case, without neglecting aspects that concern their interpretation.

3.1 Nonparametric Simplicial-Real model

As when dealing with real covariates, linear models may be too restrictive to provide an accurate fit to the responses. In such situations, data-driven perspective emerges as an alternative to parametric-driven modeling and in this new context, nonparametric regression models provide a flexible tool since now the regression function is not restricted to lie in a finite-dimensional space.

[Di Marzio et al. \(2015\)](#) introduced nonparametric estimators of the regression function by adapting the ideas developed in the Euclidean real space. As we will see, the estimators depend on weighted means and hence, they are not protected from outliers, motivating our proposals.

In the sequel, we briefly overview the proposals given by [Di Marzio et al. \(2015\)](#). Throughout this section, we assume that we have a random sample (y_i, \mathbf{x}_i) , $1 \leq i \leq n$, such that $y_i \in \mathbb{R}$, $\mathbf{x}_i \sim \mathcal{S}^D$ and $(y_i, \mathbf{x}_i) \sim (Y, \mathbf{X})$ where (Y, \mathbf{X}) satisfies the regression model

$$Y = m(\mathbf{X}) + \sigma(\mathbf{X})\epsilon, \tag{6}$$

where the error ϵ is independent of the simplicial covariates \mathbf{X} and have a symmetric distribution $F_0(\cdot)$, that is, we assume that the error's scale equals 1 to identify the scale function. Hence, when second

moments exist, we have that $\mathbb{E}(Y|\mathbf{X}) = m(\mathbf{X})$ and $\sigma^2(\mathbf{X}) = \mathbb{E}((Y - m(\mathbf{X}))^2|\mathbf{X})$ is the conditional variance function.

3.2 The classical approaches

To define nonparametric regression estimators, [Di Marzio et al. \(2015\)](#) introduced simplicial kernels as follows. Kernels were introduced in [Aitchison and Lauder \(1985\)](#) and [Chacón et al. \(2011\)](#) in the framework of density estimation on the simplex.

Let \mathcal{K} be a continuous even function with maximum at 0 such that $\int \mathcal{K}(x)dx < \infty$. The D -simplicial kernel can be defined as

$$K(\mathbf{u}) = \frac{\mathcal{K}(\|\mathbf{u}\|_a)}{\int_{\mathbb{R}^D} \mathcal{K}(\|\mathbf{u}\|_a) d\lambda_a(\mathbf{u})},$$

where $\|\mathbf{u}\|_a$ stands for $\|\mathbf{u}\|_a = \|\mathbf{u}^*\|$ and λ_a is the Aitchison measure introduced above. Then, we have

$$K(\mathbf{u}) = \tilde{K}(\mathbf{u}^*) = \frac{\mathcal{K}(\|\mathbf{u}^*\|)}{\int_{\mathbb{R}^{D-1}} \mathcal{K}(\|\mathbf{u}^*\|) d\mathbf{u}^*}.$$

The kernel K is a density on \mathcal{S}^D with respect to the Aitchison measure, whereas \tilde{K} is a density on \mathbb{R}^{D-1} with respect to the Lebesgue measure.

As mentioned in [Di Marzio et al. \(2015\)](#), the kernel defined through $K(\mathbf{u}) = \tilde{K}(\mathbf{u}^*)$ is invariant when changing the orthonormal basis for \mathcal{S}^D , for that reason, henceforth, we will consider the following explicit expression of the *ilr*-transformation

$$u_j^* = \sqrt{\frac{j}{j+1}} \log \left\{ \frac{g_j(u_1, \dots, u_j)}{u_{j+1}} \right\}, \quad (7)$$

where $\mathbf{u}^* = \text{ilr}(\mathbf{u}) = (u_1^*, \dots, u_{D-1}^*)^\top$ and $g_j(u_1, \dots, u_j) = \left(\prod_{\ell=1}^j u_\ell \right)^{1/j}$ is the geometric mean of components of (u_1, \dots, u_j) . Note that this transformation is the one considered in [Egozcue et al. \(2003\)](#) and [Chacón et al. \(2011\)](#).

Given a symmetric positive definite matrix $\mathbf{H} \in \mathbb{R}^{(D-1) \times (D-1)}$ and $\mathbf{u} \in \mathcal{S}^D$, a simplicial kernel centered at $\mathbf{x} \in \mathcal{S}^D$ and rescaled by \mathbf{H} , is defined as

$$K_{\mathbf{H}}(\mathbf{u} \ominus \mathbf{x}) = \frac{1}{\det(\mathbf{H})} \tilde{K}(\mathbf{H}^{-1}(\mathbf{u}^* - \mathbf{x}^*)) = \tilde{K}_{\mathbf{H}}(\mathbf{u}^* - \mathbf{x}^*). \quad (8)$$

[Di Marzio et al. \(2015\)](#) introduced a local constant estimator for $m(\mathbf{x})$ as the minimizer of $\sum_{i=1}^n (y_i - b)^2 K_{\mathbf{H}}(\mathbf{x}_i \ominus \mathbf{x})$, which leads to the following expression for the resulting estimator $\hat{m}(\mathbf{x}) = \frac{\sum_{i=1}^n w_i(\mathbf{x}) y_i}{\sum_{i=1}^n w_i(\mathbf{x})}$, where

$$w_i(\mathbf{x}) = K_{\mathbf{H}}(\mathbf{x}_i \ominus \mathbf{x}) \left\{ \sum_{j=1}^n K_{\mathbf{H}}(\mathbf{x}_j \ominus \mathbf{x}) \right\}^{-1}. \quad (9)$$

The local linear version of this estimator is defined as $\hat{m}(\mathbf{x}) = \hat{b}_0$, where

$$(\hat{b}_0, \hat{\mathbf{b}}_1) = \underset{(b_0, \mathbf{b}_1): \mathbf{b}_1^\top \mathbf{1}_D = 0}{\operatorname{argmin}} \sum_{i=1}^n \left\{ y_i - b_0 - \mathbf{b}_1^\top \log(\mathbf{x}_i \ominus \mathbf{x}) \right\}^2 K_{\mathbf{H}}(\mathbf{x}_i \ominus \mathbf{x}) = \underset{(b_0, \mathbf{b}_1): \mathbf{b}_1^\top \mathbf{1}_D = 0}{\operatorname{argmin}} L_n(b_0, \mathbf{b}_1, \mathbf{x}).$$

Recall that we have defined the hyperplane \mathcal{V} as $\mathcal{V} = \{\mathbf{z} \in \mathbb{R}^D : \sum_{j=1}^D z_j = 0\}$. Since $\mathbf{b}_1 \in \mathcal{V}$, we have that $L_n(b_0, \mathbf{b}_1, \mathbf{x}) = \sum_{i=1}^n \{y_i - b_0 - \langle \text{inv.clr}(\mathbf{b}_1), \mathbf{x}_i \ominus \mathbf{x} \rangle_a\}^2 K_{\mathbf{H}}(\mathbf{x}_i \ominus \mathbf{x})$. Hence the estimator can be viewed as a local linear smoother with respect to the natural Aitchison geometry in the simplex.

As mentioned in [Di Marzio et al. \(2015\)](#), the loss $L_n(b_0, \mathbf{b}_1, \mathbf{x})$ may be re-written using the *ilr*-transformation as

$$\sum_{i=1}^n \left\{ y_i - b_0 - \mathbf{b}_1^{\top} (\mathbf{x}_i^* - \mathbf{x}^*) \right\}^2 \tilde{K}_{\mathbf{H}} (\mathbf{x}_i^* - \mathbf{x}^*),$$

which leads to an explicit expression for the local linear estimator as

$$\hat{m}(\mathbf{x}) = \mathbf{i}_1^{\top} \left(\mathbb{X}^{\top} \mathbb{K} \mathbb{X} \right)^{-1} \mathbb{X}^{\top} \mathbb{K} \mathbb{Y}, \quad (10)$$

where \mathbf{i}_1 is the first canonical vector in \mathbb{R}^D , that is, the vector having its first component equal to 1 and the remaining ones equal to 0, $\mathbb{K} = \text{DIAG} \left(\tilde{K}_{\mathbf{H}} (\mathbf{x}_1^* - \mathbf{x}^*), \dots, \tilde{K}_{\mathbf{H}} (\mathbf{x}_n^* - \mathbf{x}^*) \right)$,

$$\mathbb{Y} = (y_1, \dots, y_n)^{\top} \quad \text{and} \quad \mathbb{X} = \begin{pmatrix} 1 & (\mathbf{x}_1^* - \mathbf{x}^*)^{\top} \\ \vdots & \vdots \\ 1 & (\mathbf{x}_n^* - \mathbf{x}^*)^{\top} \end{pmatrix}. \quad (11)$$

As mentioned, equation (10) shows that the resulting estimators are a weighted mean of the responses and from this fact it becomes evident that the estimator may be very sensitive to outliers among y_i . In this sense, one could make the estimator to take an arbitrarily large value just by choosing an appropriate atypical response. In the next section we propose a robust alternative that will be much more stable in presence of anomalous data among the responses.

3.3 The robust estimators

To robustify the local constant and local linear kernel estimators under the simplicial-real regression model (6) one may consider an M -smoother with the kernel weights defined above.

More precisely, as in the Euclidean case, define the empirical conditional distribution function $\hat{F}(y|\mathbf{X} = \mathbf{x})$ as

$$\hat{F}(y|\mathbf{X} = \mathbf{x}) = \sum_{i=1}^n w_i(\mathbf{x}) \mathbb{I}_{(-\infty, y]}(y_i), \quad (12)$$

with $w_i(\mathbf{x})$ the kernel weights defined in (9). Note that, as above, this estimator can be computed using the *ilr*-transformation as

$$\hat{F}(y|\mathbf{X} = \mathbf{x}) = \sum_{i=1}^n \tilde{w}_i(\mathbf{x}^*) \mathbb{I}_{(-\infty, y]}(y_i),$$

where

$$\tilde{w}_i(\mathbf{x}^*) = \tilde{K}_{\mathbf{H}} (\mathbf{x}_i^* - \mathbf{x}^*) \left\{ \sum_{j=1}^n \tilde{K}_{\mathbf{H}} (\mathbf{x}_j^* - \mathbf{x}^*) \right\}^{-1}, \quad (13)$$

since (8) implies that $w_i(\mathbf{x}) = \tilde{w}_i(\mathbf{x}^*)$, where $\mathbf{x}^* = \text{ilr}(\mathbf{x})$.

As it is well known, to decide which observations may be considered as atypical, the size of the residuals should be measured with respect to some appropriate scale or dispersion measure, see for instance, Sections 2.6 and 6.9.1 in [Maronna et al. \(2019\)](#). For that reason, the first step to define robust estimators of the regression function is to introduce a robust scale.

Define $\hat{m}_{\text{INI}}(\mathbf{x})$ the local median, that is, the median of the empirical conditional distribution function $\hat{F}(y|\mathbf{X} = \mathbf{x})$. Take a preliminary robust scale estimator $\hat{\sigma}(\mathbf{x})$, such as the local MAD, that

is, the median of the empirical conditional distribution of the absolute value of the residuals $\widehat{r}_{i,\mathbf{x}} = y_i - \widehat{m}_{\text{INI}}(\mathbf{x})$, which is computed as

$$\widehat{G}(r|\mathbf{X} = \mathbf{x}) = \sum_{i=1}^n w_i(\mathbf{x}) \mathbb{I}_{(-\infty, r]}(|\widehat{r}_{i,\mathbf{x}}|).$$

Other possible choices for $\widehat{\sigma}(\mathbf{x})$ are local S -scale estimators. To define them, as in [Maronna et al. \(2019\)](#), let $\rho : \mathbb{R} \rightarrow \mathbb{R}_+$ be a bounded ρ -function, that is, an even function, non-decreasing on $|r|$, increasing for $r > 0$ when $\rho(r) < \lim_{r \rightarrow +\infty} \rho(r)$ and such that $\rho(0) = 0$. The local S -scale estimator $\widehat{\sigma}(\mathbf{x})$ is defined as the solution in s of

$$\sum_{i=1}^n w_i(\mathbf{x}) \rho_{c_0} \left(\frac{\widehat{r}_{i,\mathbf{x}}}{s} \right) = b,$$

where $\rho_c(r) = \rho(r/c)$, and $c_0 > 0$ is a user-chosen tuning constant. When ρ is the Tukey's biweight function, $\rho(r) = \min(3r^2 - 3r^4 + r^6, 1)$, the choice $c = 1.54764$ and $b = 1/2$ ensures that the estimator is Fisher-consistent for normal errors. Note that the local MAD corresponds to the choice $\rho(r) = \mathbb{I}_{(1,\infty)}(|r|)$, $c = 1$ and $b = 0.5$.

When the model is homocedastic, a global robust scale estimator $\widehat{\sigma}$ may be computed as the solution in s of

$$\sum_{i=1}^n \rho_{c_0} \left(\frac{\widehat{r}_i}{s} \right) = b, \tag{14}$$

where $\widehat{r}_i = y_i - \widehat{m}_{\text{INI}}(\mathbf{x}_i)$. Consistency of these scale estimators for Euclidean covariates were given in [Boente and Martinez \(2017\)](#). Moreover, for Euclidean covariates, local M -smoothers were studied, among others in [Härdle and Tsybakov \(1988\)](#) and [Boente and Fraiman \(1989\)](#), while robust local linear smoothers were considered in [Cleveland \(1979\)](#) and [Jiang and Mack \(2001\)](#).

In the definitions to be given below, it should be taking into account that if the model is homocedastic, a robust scale estimator $\widehat{\sigma}$ should be used instead of the local one $\widehat{\sigma}(\mathbf{x})$.

Inspired in these approaches, we propose the following estimators:

- Local M -smoothers may be defined using a loss function ρ_{c_1} where $c_1 > c_0$ as the minimizer $\widehat{m}(\mathbf{x})$ of $\widehat{\gamma}(\mathbf{x}, a, \widehat{\sigma}(\mathbf{x}))$, where

$$\widehat{\gamma}_j(\mathbf{x}, a, \varsigma) = \sum_{i=1}^n w_i(\mathbf{x}) \rho_{c_1} \left(\frac{y_i - a}{\varsigma} \right). \tag{15}$$

It is worth mentioning that if ρ is differentiable, $\psi = \rho'$ and $\psi_c(t) = \psi(t/c)$, then $\widehat{m}(\mathbf{x})$ is the solution of $\widehat{\lambda}(\mathbf{x}, \widehat{m}(\mathbf{x}), \widehat{\sigma}(\mathbf{x})) = 0$, with

$$\widehat{\lambda}(\mathbf{x}, a, \varsigma) = \sum_{i=1}^n w_i(\mathbf{x}) \psi_{c_1} \left(\frac{y_i - a}{\varsigma} \right). \tag{16}$$

Furthermore, if ψ is an increasing function (16) has a unique solution. In contrast, when considering a bounded ρ -function, the algorithm provided below provides a procedure to obtain a consistent estimator.

- Local linear M -smoothers may be defined as follows. Let ρ_{c_1} be a ρ -function such that $c_1 > c_0$ and define

$$(\widehat{b}_0, \widehat{\mathbf{b}}_1) = \underset{(b_0, \mathbf{b}_1) : \mathbf{b}_1^\top \mathbf{1}_D = 0}{\operatorname{argmin}} \sum_{i=1}^n w_i(\mathbf{x}) \rho_{c_1} \left(\frac{y_i - b_0 - \mathbf{b}_1^\top \log(\mathbf{x}_i \ominus \mathbf{x})}{\widehat{\sigma}(\mathbf{x})} \right).$$

Then, $\widehat{m}(\mathbf{x}) = \widehat{b}_0$. As in the classical case, using the *ilr*-transformation, we have that $\widehat{m}(\mathbf{x}) = \widehat{b}_0$, where

$$(\widehat{b}_0, \widehat{\mathbf{b}}_1^*) = \underset{(b_0, \mathbf{b}_1^*)}{\operatorname{argmin}} \sum_{i=1}^n \widetilde{w}_i(\mathbf{x}^*) \rho_{c_1} \left(\frac{y_i - b_0 - \mathbf{b}_1^{*\top}(\mathbf{x}_i^* - \mathbf{x}^*)}{\widehat{\sigma}(\mathbf{x})} \right),$$

with $\mathbf{x}^* = \operatorname{ilr}(\mathbf{x})$. Note that $(\widehat{b}_0, \widehat{\mathbf{b}}_1^*)$ satisfy

$$\sum_{i=1}^n \widetilde{w}_i(\mathbf{x}^*) \psi_{c_1} \left(\frac{y_i - \widehat{b}_0 - \widehat{\mathbf{b}}_1^{*\top}(\mathbf{x}_i^* - \mathbf{x}^*)}{\widehat{\sigma}(\mathbf{x})} \right) \begin{pmatrix} 1 \\ \mathbf{x}_i^* - \mathbf{x}^* \end{pmatrix} = \mathbf{0},$$

which suggests a reweighted version of the algorithm used to compute M -estimators, that will be described below. Indeed, defining $W_{c_1}(t) = \psi_{c_1}(t)/t$ and the standardized residuals

$$\widehat{r}_{i,\mathbf{x}} = \frac{y_i - \widehat{b}_0 - \widehat{\mathbf{b}}_1^{*\top}(\mathbf{x}_i^* - \mathbf{x}^*)}{\widehat{\sigma}(\mathbf{x})},$$

and the matrix

$$\widehat{\mathbf{B}}_{\mathbf{x}} = \sum_{i=1}^n \widetilde{w}_i(\mathbf{x}^*) W_{c_1}(\widehat{r}_{i,\mathbf{x}}) \begin{pmatrix} 1 \\ \mathbf{x}_i^* - \mathbf{x}^* \end{pmatrix} \begin{pmatrix} 1 \\ \mathbf{x}_i^* - \mathbf{x}^* \end{pmatrix}^\top,$$

we have that

$$\begin{pmatrix} \widehat{b}_0 \\ \widehat{\mathbf{b}}_1^{*\top} \end{pmatrix} = \widehat{\mathbf{B}}_{\mathbf{x}}^{-1} \sum_{i=1}^n \widetilde{w}_i(\mathbf{x}^*) W_{c_1}(\widehat{r}_{i,\mathbf{x}}) \begin{pmatrix} 1 \\ \mathbf{x}_i^* - \mathbf{x}^* \end{pmatrix} y_i.$$

Note that, if we define the matrix $\widehat{\mathbb{K}} = \operatorname{DIAG}(\widetilde{w}_1(\mathbf{x}^*) W_{c_1}(\widehat{r}_{1,\mathbf{x}}), \dots, \widetilde{w}_n(\mathbf{x}^*) W_{c_1}(\widehat{r}_{n,\mathbf{x}}))$, we have that $\widehat{m}(\mathbf{x})$ satisfies $\widehat{m}(\mathbf{x}) = \mathbf{i}_1^\top \left(\mathbb{X}^\top \widehat{\mathbb{K}} \mathbb{X} \right)^{-1} \mathbb{X}^\top \widehat{\mathbb{K}} \mathbb{Y}$, an expression closely related to (10), except that the matrix $\widehat{\mathbb{K}}$ involves the estimators $(\widehat{b}_0, \widehat{\mathbf{b}}_1^*)$. This is the basis for the algorithm described in Algorithm 2.

Taking into account that $w_i(\mathbf{x}) = \widetilde{w}_i(\operatorname{ilr}(\mathbf{x}))$, local M -smoothers may be numerically computed using the following algorithm.

Algorithm 1 The robust local M -smoother

- 1: Let $\ell = 0$ and $\widehat{m}^{(0)} = \widehat{m}_{\operatorname{INI}}(\mathbf{x})$ be the local median and let $\widehat{\sigma}(\mathbf{x})$ be a robust local scale estimator, as the one defined in (14). Furthermore, let $\widetilde{w}_i(\mathbf{x}^*)$ be defined as in (13), with $\mathbf{x}^* = \operatorname{ilr}(\mathbf{x})$
 - 2: **repeat**
 - 3: $\ell \leftarrow \ell + 1$
 - 4: **for** $i = 1$ **to** n **do**
 - 5: Let $\widehat{r}_i(\mathbf{x})$ be the standardized residuals $\widehat{r}_i(\mathbf{x}) = (y_i - \widehat{m}^{(\ell)}(\mathbf{x}))/\widehat{\sigma}(\mathbf{x})$ and $W_i^{(\ell)} = \widetilde{w}_i(\mathbf{x}^*) W_{c_1}(\widehat{r}_i(\mathbf{x}))$.
 - 6: **end for**
 - 7: Let $\widehat{m}^{(\ell+1)}(\mathbf{x}) = \sum_{i=1}^n W_i^{(\ell)} y_i / \sum_{i=1}^n W_i^{(\ell)}$.
 - 8: **until** convergence
-

Similarly, M -local linear estimators may be computed through

Algorithm 2 The robust local linear M -smoother

- 1: Define the matrices \mathbb{Y} and \mathbb{X} as in (11).
- 2: Let $\ell = 0$ and take $\widehat{b}_0^{(0)} = \widehat{m}_{\text{INI}}(\mathbf{x})$ the local median, $\widehat{\mathbf{b}}_1^{*(0)} = \mathbf{0}_{D-1}$ and let $\widehat{\sigma}(\mathbf{x})$ be a robust local scale estimator, as the one defined in (14). Furthermore, let $\widetilde{w}_i(\mathbf{x}^*)$ be defined as in (13), with $\mathbf{x}^* = \text{ilr}(\mathbf{x})$
- 3: **repeat**
- 4: $\ell \leftarrow \ell + 1$
- 5: **for** $i = 1$ **to** n **do**
- 6: Let $\widehat{r}_i(\mathbf{x})$ be the standardized residuals

$$\widehat{r}_i(\mathbf{x}) = \frac{y_i - \widehat{b}_0^{(\ell)} - \widehat{\mathbf{b}}_1^{*(\ell)\top}(\mathbf{x}_i^* - \mathbf{x}^*)}{\widehat{\sigma}(\mathbf{x})}$$

and $W_i^{(\ell)} = \widetilde{w}_i(\mathbf{x}^*) W_{c_1}(\widehat{r}_i(\mathbf{x}))$.

- 7: **end for**
- 8: Define the matrix

$$\widehat{\mathbb{K}}^{(\ell)} = \text{DIAG} \left(W_1^{(\ell)}, \dots, W_n^{(\ell)} \right),$$

- 9: Let $(\widehat{b}_0^{(\ell+1)}, \widehat{\mathbf{b}}_1^{*(\ell+1)\top})^\top = \left(\mathbb{X}^\top \widehat{\mathbb{K}}^{(\ell)} \mathbb{X} \right)^{-1} \mathbb{X}^\top \widehat{\mathbb{K}} \mathbb{Y}$ and $\widehat{m}^{(\ell+1)}(\mathbf{x}) = \widehat{b}_0^{(\ell+1)}$
 - 10: **until** convergence
-

3.4 Selection of the bandwidth parameter

As with other non-parametric procedures, the selection of the smoothing parameter is an important practical issue when fitting additive models. The importance of using a robust criterion for selecting smoothing parameters, even when one uses robust estimators, has been extensively described, see for instance Leung et al. (1993), Wang and Scott (1994), Boente et al. (1997), Cantoni and Ronchetti (2001) and Leung (2005). Several proposals have been made in the literature, including L^1 -cross-validation (Wang and Scott, 1994), robust versions of C_p and cross-validation (Cantoni and Ronchetti, 2001; Bianco and Boente, 2007) and a robust plug-in procedure discussed in Boente et al. (1997).

As in Di Marzio et al. (2015), we will consider the case where the bandwidth matrix \mathbf{H} equals $h \mathbf{I}_{D-1}$. In such a case, the parameter h may be chosen using a robust leave-one-out cross-validation criterion, see Bianco and Boente (2007) and Boente and Rodriguez (2008) or more generally a K -fold cross-validation procedure. To define the robust selection method, given the sample (y_i, \mathbf{x}_i) , $1 \leq i \leq n$, denote $\widehat{m}_h^{(-i)}(\mathbf{x})$ the regression estimator computed with bandwidth h using all the data except (y_i, \mathbf{x}_i) and define the cross-validation residual $\widehat{\epsilon}_i(h) = y_i - \widehat{m}_h^{(-i)}(\mathbf{x}_i)$. The classical cross-validation criterion considered in Di Marzio et al. (2015) obtains adaptive data-driven bandwidths, by minimizing

$$CV(h) = \frac{1}{n} \sum_{i=1}^n \widehat{\epsilon}_i(h)^2 = \frac{1}{n} \sum_{i=1}^n \left(\widehat{\epsilon}_i(h) - \frac{1}{n} \sum_{\ell=1}^n \widehat{\epsilon}_\ell(h) \right)^2 + \left(\frac{1}{n} \sum_{\ell=1}^n \widehat{\epsilon}_\ell(h) \right)^2. \quad (17)$$

Bianco and Boente (2007), following Leung et al. (1993), suggests to replace the square function by a ρ -function after scaling the residuals to control the effect of large responses in partly linear autoregression models. These authors notice that this procedure lacks of robustness when using the the Huber's ρ functions due to its unboundness, while the performance of the criterion based on Tukey's ρ -function, is similar to that attained by a method which replaces the square function by the square of Huber's score function. The robust cross-validation criterion to be defined below is based on the idea that in (17) the right hand side is decomposed into the sum of the squared bias and the

variance, leading to an objective function that tries to measure both bias and variance. Based on this property, Bianco and Boente (2007) suggested a new procedure that establishes a trade-off between robust measures of bias and dispersion instead and that, according to their simulation study, turn out to be preferable than those based on bounding the squared residuals. In the actual framework we will follow these ideas to provide a robust data-driven bandwidth in regression models with compositional data. For that purpose, let $\mu_n(z_1, \dots, z_n)$ and $s_n(z_1, \dots, z_n)$ denote robust estimators of location and dispersion based on the sample $\{z_1, \dots, z_n\}$, respectively. Possible location estimator, μ_n , may be the median, while s_n can be taken as the MAD, the bisquare a-scale estimator or the Huber τ -scale estimator. A robust cross-validation criterion can be defined by minimizing on h the quantity

$$RCV(h) = \mu_n^2(\hat{\epsilon}_1(h), \dots, \hat{\epsilon}_n(h)) + s_n^2(\hat{\epsilon}_1(h), \dots, \hat{\epsilon}_n(h)). \quad (18)$$

Another possibility is to consider a K -fold cross-validation method. For that purpose, first randomly partition the data set into K disjoint subsets of approximately equal sizes, with indices \mathcal{C}_j , $1 \leq j \leq K$, so that $\bigcup_{j=1}^K \mathcal{C}_j = \{1, \dots, n\}$. Let $\mathcal{H} \subset \mathbb{R}$ be the set of bandwidth combinations to be considered, and let $\hat{m}_h^{(-j)}(\mathbf{x})$ be the robust estimator of $m(\mathbf{x})$ computed with the smoothing parameter $h \in \mathcal{H}$ and without using the observations with indices in \mathcal{C}_j . For each $i = 1, \dots, n$, define as above the residuals $\hat{\epsilon}_i(h)$ as

$$\hat{\epsilon}_i(h) = y_i - \hat{m}_h^{(-j)}(\mathbf{x}_i), \quad i \in \mathcal{C}_j, \quad j = 1, \dots, K.$$

The robust K -fold cross-validation bandwidth parameter h is selected by minimizing over $h \in \mathcal{H}$ the following criterion:

$$RCV_K(h) = \mu_n^2(\hat{\epsilon}_1(h), \dots, \hat{\epsilon}_n(h)) + s_n^2(\hat{\epsilon}_1(h), \dots, \hat{\epsilon}_n(h)). \quad (19)$$

Note that when $K = n$ and $\mathcal{C}_j = \{j\}$, $1 \leq j \leq n$, $RCV_K(h)$ equals the leave-one-out version of the robust cross-validation criterion defined through (18).

4 Monte Carlo study

This section contains the results of a simulation study conducted to compare, under different models and contamination schemes, the performance of the robust estimators defined in Section 3.3 with their classical competitors based on least squares. All computations were carried out in R.

The classical estimators are labelled CL_0 and CL_1 when using the local mean or the local linear estimator introduced in Di Marzio et al. (2015). For the robust estimators, we first compute the scale estimator using an S -scale as described in Section 3.3 using the Tukey's bisquare function with tuning constants $c_0 = 1.54764$ and $b = 1/2$, since the model is homoscedastic. The local M -smoother, labelled ROB_0 , was computed using the Tukey's bisquare function with tuning constant $c_1 = 4.685$. As mentioned above, the value $c_0 = 1.54764$ ensures Fisher-consistency of the scale estimator when the errors have a normal distribution.

In all scenarios, we performed $N = 500$ replications, the sample size was $n = 100$.

The samples $\{(y_i, \mathbf{x}_i)\}_{i=1}^n$ are generated with the same distribution as (Y, \mathbf{X}) , $\mathbf{X} = (X_1, X_2, X_3)^\top \in \mathcal{S}^3$. In all cases, the response and the covariates are related through the nonparametric model $Y = m(\mathbf{X}) + \sigma\epsilon$, where $\sigma = 1$, $m(\mathbf{x}) = \sin(\langle \mathbf{x}, \mathbf{b} \rangle_a)$, where $\mathbf{b} = (0.05920067, 0.7193872, 0.2214121)$. The covariates were generated using a Dirichlet distribution with parameter $\boldsymbol{\alpha} = (5, 7, 1)^\top$ or $\boldsymbol{\alpha} = (5, 7, 4)^\top$. For clean samples, denoted from now on as C_0 , the errors have a standardized normal distribution, $\epsilon \sim N(0, 1)$. For this numerical study we choose the bandwidth matrix \mathbf{H} as $\mathbf{H} = 2\mathbf{I}_{D-1}$ when $\boldsymbol{\alpha} = (5, 7, 1)^\top$ and $\mathbf{H} = \mathbf{I}_{D-1}$ when $\boldsymbol{\alpha} = (5, 7, 4)^\top$.

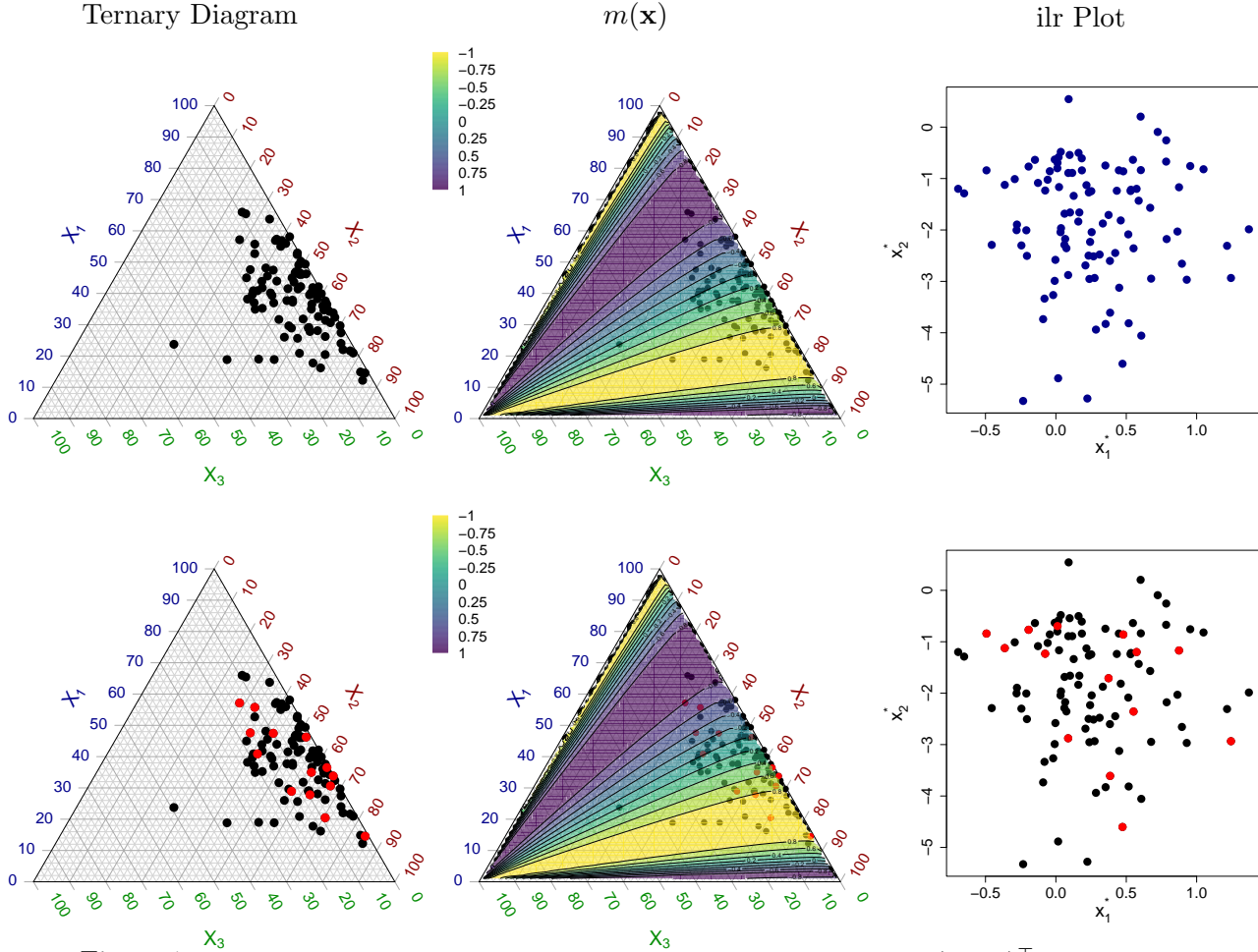


Figure 1: Synthetic data for one of the considered replications when $\alpha = (5, 7, 1)^\top$: the left panel corresponds to the ternary diagram, the middle one represents the contour plot of the regression function with the data overlaid and the right one to the transformed data. The lower panels display in red the covariates corresponding to the vertical outliers.

To study the effect of atypical data on the estimators, we considered a contamination scheme denoted $C_{1,\delta,\mu}$, which is obtained generating the errors according to $\epsilon_i \sim (1 - \delta)N(0, 1) + \delta N(\mu, 0.1^2)$. We choose $\delta = 0.10$ and $\mu = 5, 10$.

The panels in Figures 1 and 2 illustrate the shape of the covariates in one generated sample when $\alpha = (5, 7, 1)^\top$ and $\alpha = (5, 7, 4)^\top$, respectively. The left panel corresponds to the ternary diagram, the middle one represents the contour plot of the regression function and the right one to the ilr transformation of the data. The lower panel indicates in red the covariates corresponding to the vertical outliers generated by $C_{1,0.10,\mu}$.

To evaluate the behaviour of the regression estimators, we measured the performance of the estimator \hat{m} through the integrated squared error (ISE). We approximate this measure by evaluating the regression function and its estimators on points $\{\mathbf{x}_s^{(0)}\}_{s=1}^M$, generated with the same distribution as the covariates. We choose $M = 100$, that is, if \hat{m}_ℓ is the estimate of the function m obtained with the ℓ -th sample ($1 \leq \ell \leq N = 1000$), we computed

$$\text{ISE} = \frac{1}{M} \sum_{s=1}^M (\hat{m}_\ell(\mathbf{x}_s) - m(\mathbf{x}_s))^2 .$$

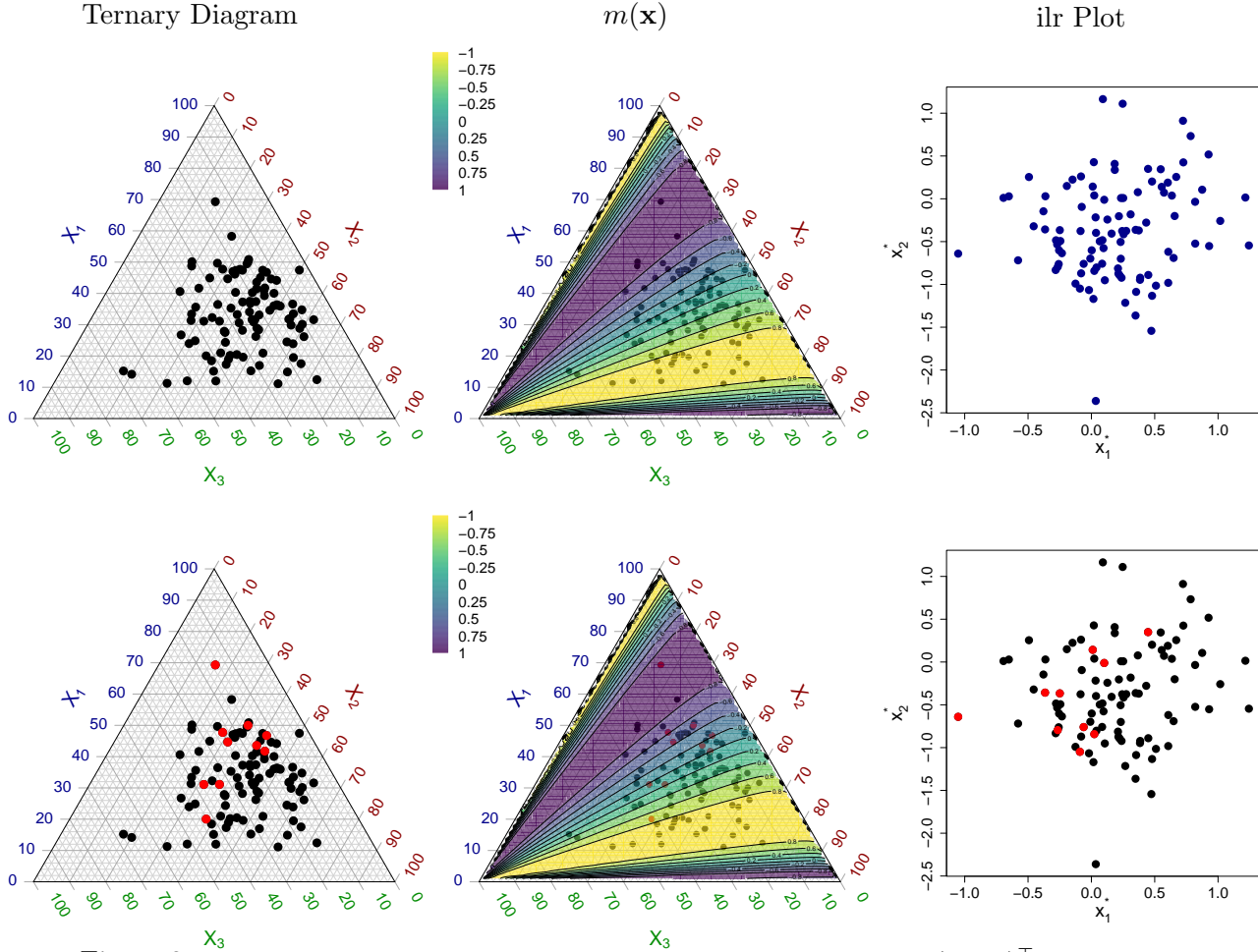


Figure 2: Synthetic data for one of the considered replications when $\alpha = (5, 7, 4)^\top$: the left panel corresponds to the ternary diagram, the middle one represents the contour plot of the regression function with the data overimposed and the right one to the transformed data. The lower panels display in red the covariates corresponding to the vertical outliers.

We also provide a measure of the global squared bias given by

$$\text{Bias}^2 = \frac{1}{M} \sum_{s=1}^M \left(\frac{1}{N} \sum_{\ell=1}^N \hat{m}_{\ell}(\mathbf{x}_s) - m(\mathbf{x}_s) \right)^2.$$

Tables 1 and 2 reports the mean over replications of the ISE, labelled MISE, and the squared bias, Bias^2 , when $\alpha = (5, 7, 1)^\top$ and $\alpha = (5, 7, 4)^\top$, respectively. The effect of the introduced vertical outliers is present on the classical procedures, in particular when $\mu = 10$. The situation $\mu = 5$ corresponds to a mild atypical data due to the considered central errors distribution and to the shape of the regression function explaining why the effect on the robust procedures is larger when $\mu = 5$ than when $\mu = 10$. However, in all cases, the robust methods described in this paper provide stable and reliable estimators. Figures 3 and 4 provide the adjusted boxplots, see Hubert and Vandervieren (2008), of the ISE. These plots show the stability of the robust procedures across contaminations and the advantage of considering local linear estimators over local constants.

To illustrate the effect of the considered contaminations on the estimators, Figures 5 to 7 depict the ternary diagram with the prediction points $\{\mathbf{x}_s^{(0)}\}_{s=1}^M$ in different colours to show an intensity plot when $\alpha = (5, 7, 1)^\top$, while Figures 8 to 10 display similar plots when $\alpha = (5, 7, 4)^\top$. The colour palette indicates the value of $\hat{m}(\mathbf{x}_s^{(0)})$ at one replication. To facilitate comparisons we present in the left panel the ternary plot where the colours identify the real function at the grid points $m(\mathbf{x}_s^{(0)})$. The warm

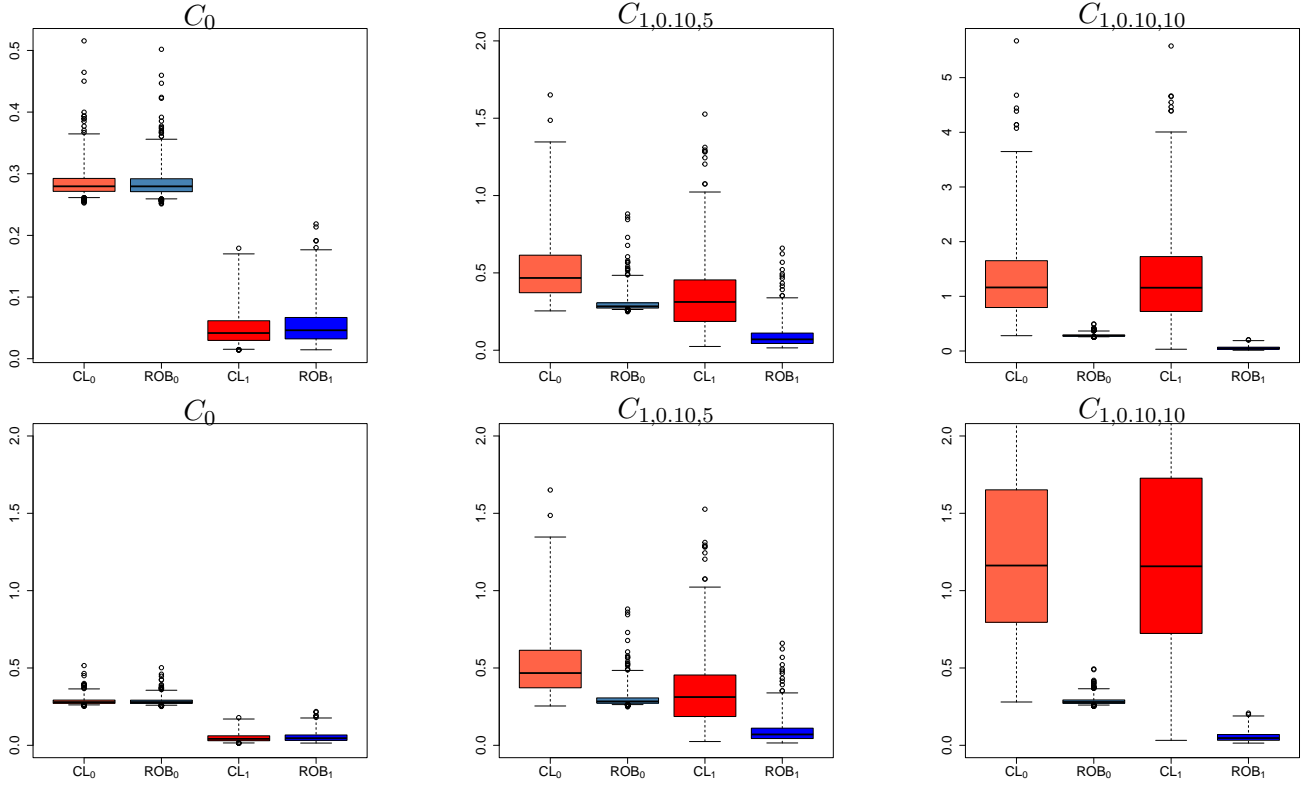


Figure 3: Adjusted boxplots of the ISE, when $\alpha = (5, 7, 1)^\top$. The second row present the boxplots in the same scale.

	MISE			Bias ²		
	C_0	$C_{1,0,10,5}$	$C_{1,0,10,10}$	C_0	$C_{1,0,10,5}$	$C_{1,0,10,10}$
CL ₀	0.2856	0.5150	1.3056	0.2721	0.4762	1.1917
CL ₁	0.0489	0.3461	1.2975	0.0156	0.2438	0.9801
ROB ₀	0.2853	0.3025	0.2869	0.2711	0.2732	0.2713
ROB ₁	0.0539	0.0892	0.0549	0.0232	0.0392	0.0198

Table 1: MISE and squared bias of the regression estimators when $\alpha = (5, 7, 1)^\top$.

	MISE			Bias ²		
	C_0	$C_{1,0,10,5}$	$C_{1,0,10,10}$	C_0	$C_{1,0,10,5}$	$C_{1,0,10,10}$
CL ₀	0.1801	0.3731	1.1058	0.1669	0.3397	1.0054
CL ₁	0.0456	0.3207	1.2212	0.0135	0.2291	0.9359
ROB ₀	0.1794	0.1838	0.1804	0.1653	0.1616	0.1655
ROB ₁	0.0481	0.0680	0.0489	0.0184	0.0262	0.0158

Table 2: MISE and squared bias of the regression estimators when $\alpha = (5, 7, 4)^\top$.

colours (red and orange) correspond to small negative values, while as the colour spectrum becomes cooler (green, blue, violet) the values of the estimators or of the true function increase to the maximum of the four procedures and 1, which is the maximum of m . The colours vary across figures due to the range of the obtained estimators, for that reason the true function is depicted in each Figure with

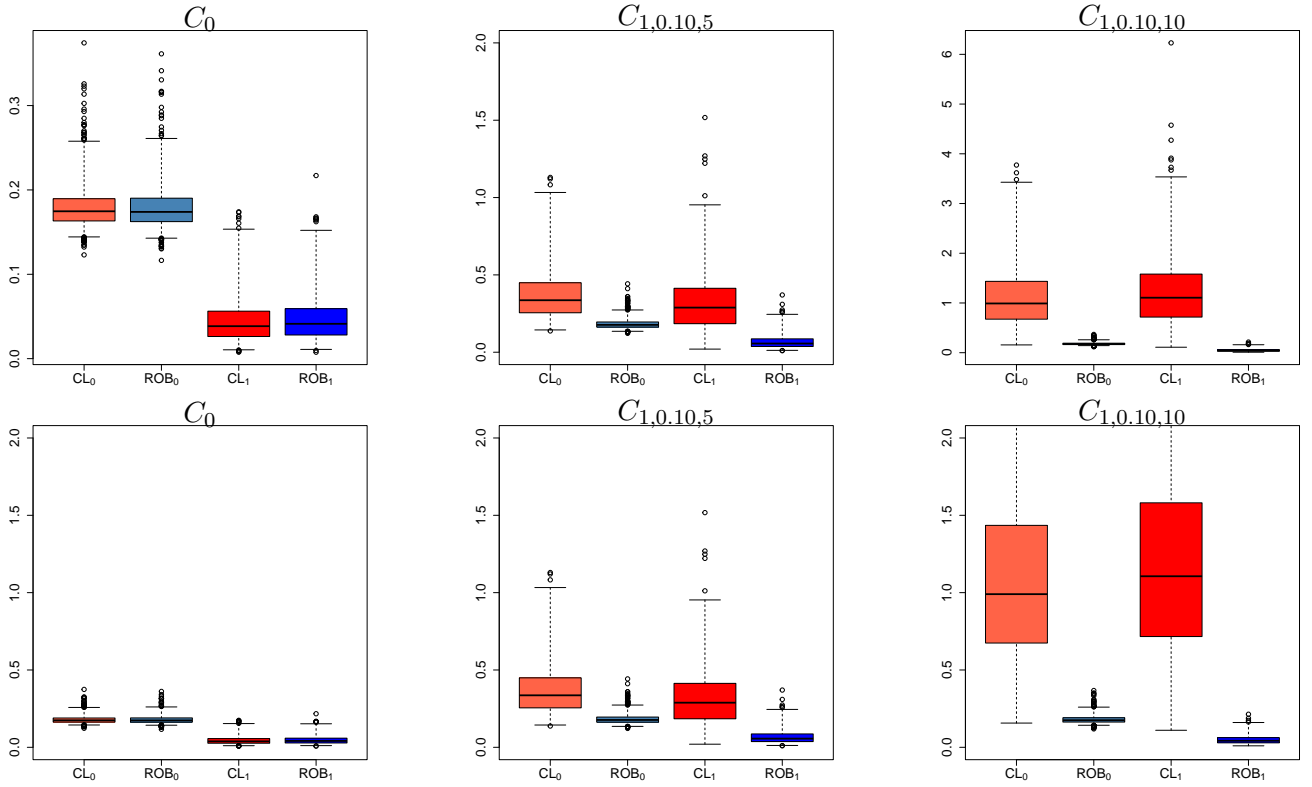


Figure 4: Adjusted boxplots of the ISE, when $\alpha = (5, 7, 4)^\top$. The second row present the boxplots in the same scale.

different colours.

As expected, for clean samples the classical and robust estimators show a similar performance, since the plots in the upper and lower rows have a similar aspect. The advantage of the local linear over the local constant is evident when comparing the middle and right panels. In effect, the right and left panels of Figure 5 are quite similar, while the middle ones lead to more biased estimators. Similar conclusions may be obtained when $\alpha = (5, 7, 4)^\top$, see Figure 8.

Figures 6 and 7 and also Figures 9 and 10 exhibit the damaging effect of vertical outliers on the classical estimators in particular, when $\mu = 10$. They also reflect the stability of the robust local lineal procedure.

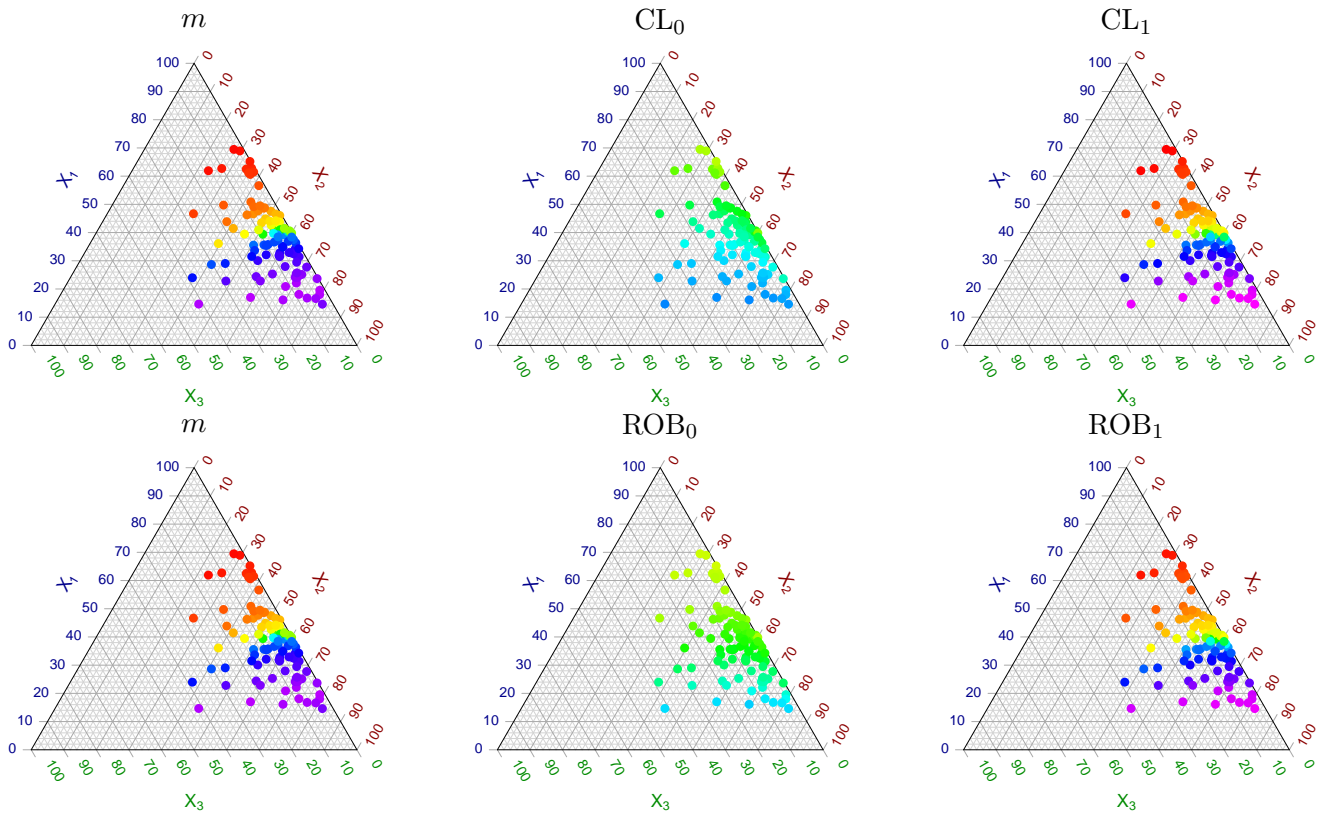


Figure 5: Ternary diagrams with the prediction points $\{\mathbf{x}_s^{(0)}\}_{s=1}^M$ in different colours when $\boldsymbol{\alpha} = (5, 7, 1)^\top$. The colour palette indicates the value of $\hat{m}(\mathbf{x}_s^{(0)})$ under C_0 and $m(\mathbf{x}_s^{(0)})$.

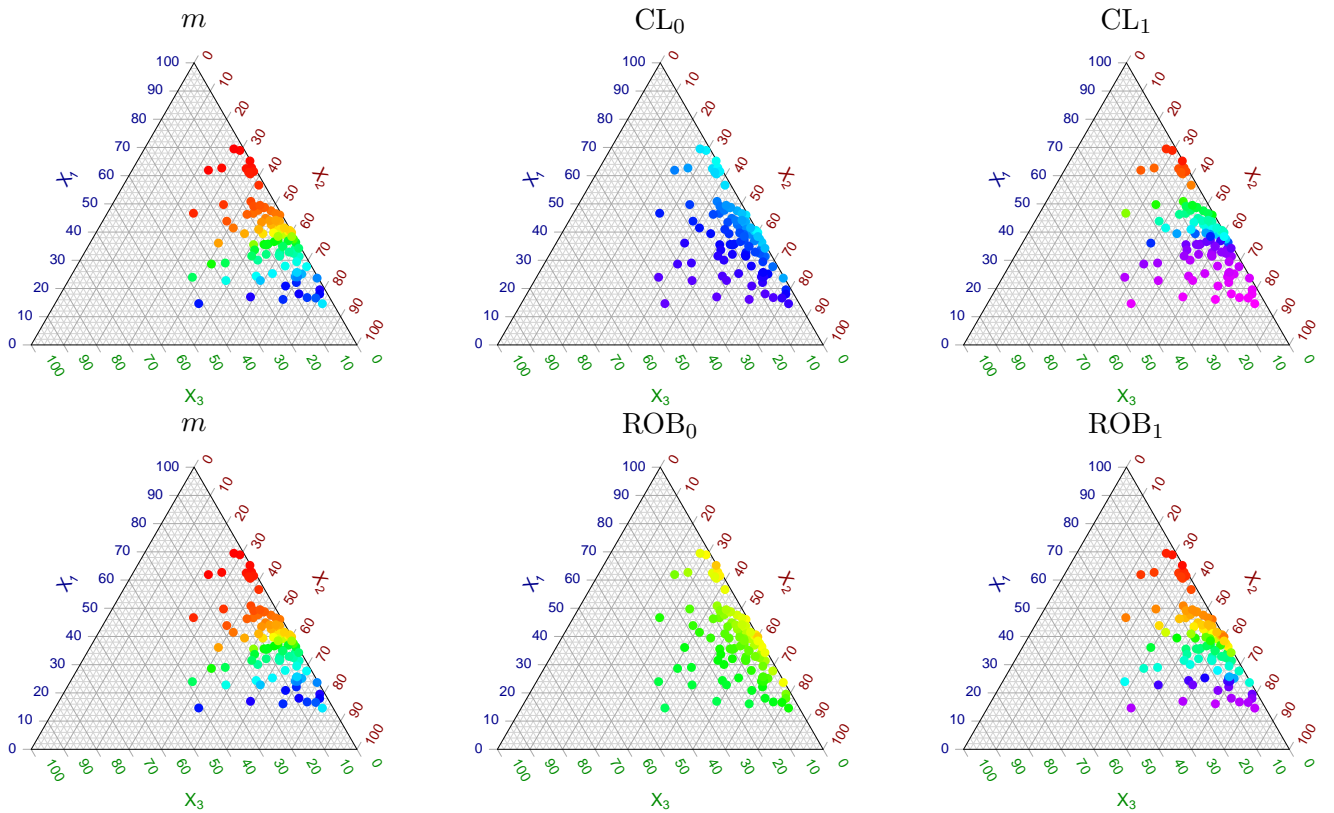


Figure 6: Ternary diagrams with the prediction points $\{\mathbf{x}_s^{(0)}\}_{s=1}^M$ in different colours, when $\boldsymbol{\alpha} = (5, 7, 1)^\top$. The colour palette indicates the value of $\hat{m}(\mathbf{x}_s^{(0)})$ under $C_{1,0,10,5}$ and $m(\mathbf{x}_s^{(0)})$.

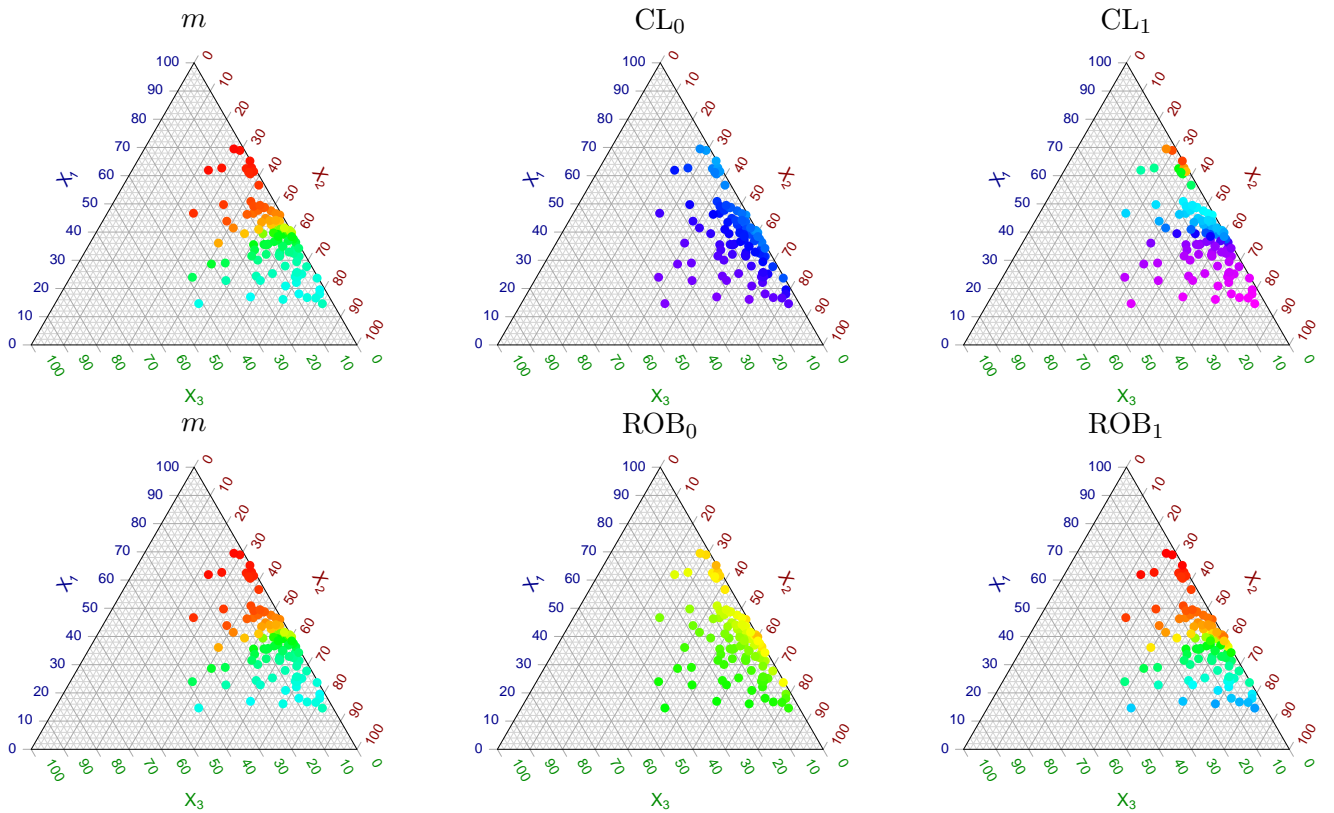


Figure 7: Ternary diagrams with the prediction points $\{\mathbf{x}_s^{(0)}\}_{s=1}^M$ in different colours, when $\boldsymbol{\alpha} = (5, 7, 1)^\top$. The colour palette indicates the value of $\hat{m}(\mathbf{x}_s^{(0)})$ under $C_{1,0.10,10}$ and $m(\mathbf{x}_s^{(0)})$.

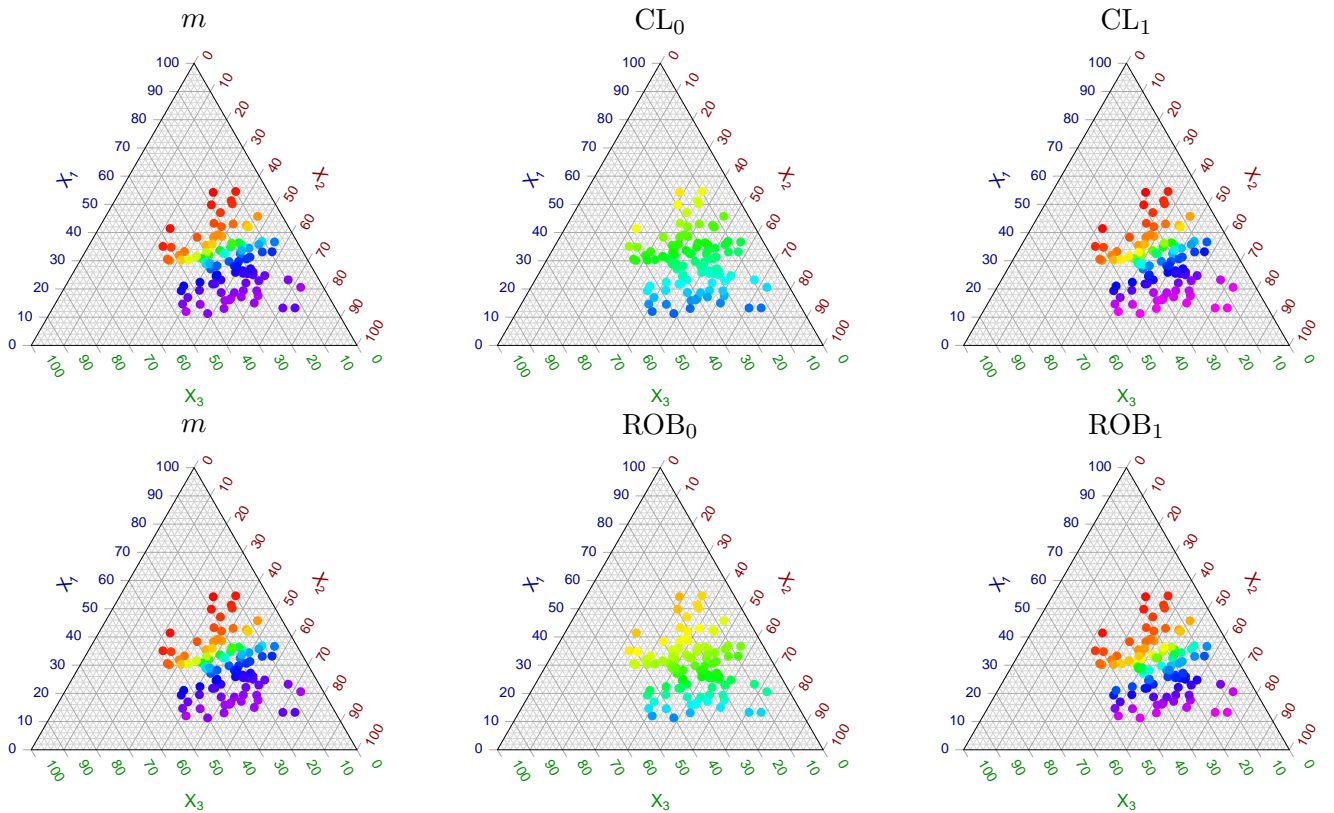


Figure 8: Ternary diagrams with the prediction points $\{\mathbf{x}_s^{(0)}\}_{s=1}^M$ in different colours, when $\alpha = (5, 7, 4)^\top$. The colour palette indicates the value of $\hat{m}(\mathbf{x}_s^{(0)})$ under C_0 and $m(\mathbf{x}_s^{(0)})$.

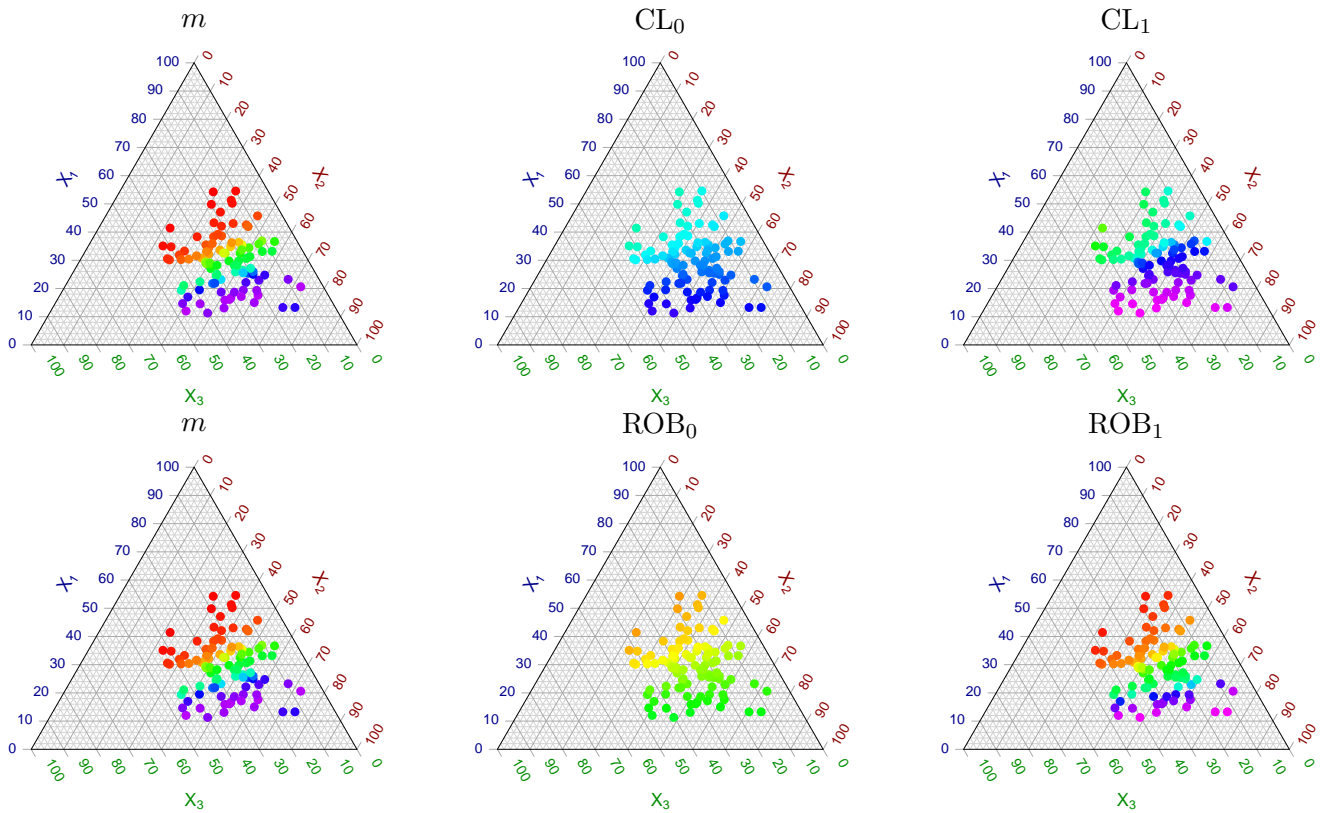


Figure 9: Ternary diagrams with the prediction points $\{\mathbf{x}_s^{(0)}\}_{s=1}^M$ in different colours, when $\boldsymbol{\alpha} = (5, 7, 4)^\top$. The colour palette indicates the value of $\hat{m}(\mathbf{x}_s^{(0)})$ under $C_{1,0.10,5}$ and $m(\mathbf{x}_s^{(0)})$.

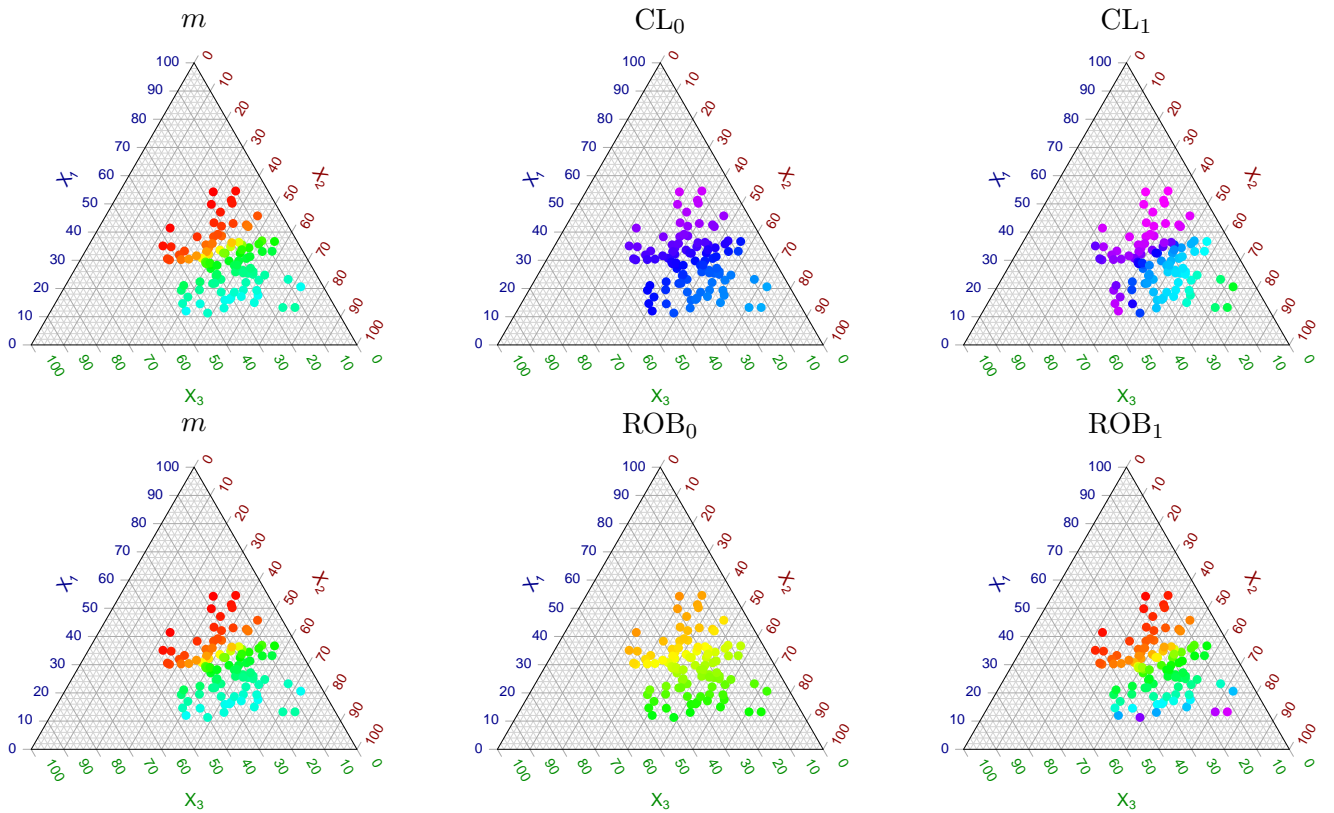


Figure 10: Ternary diagrams with the prediction points $\{\mathbf{x}_s^{(0)}\}_{s=1}^M$ in different colours, when $\alpha = (5, 7, 4)^\top$. The colour palette indicates the value of $\hat{m}(\mathbf{x}_s^{(0)})$ under $C_{1,0.10,10}$ and $m(\mathbf{x}_s^{(0)})$.

5 Real Data Analysis

Clinical studies have investigated the impact of macronutrient composition on average glucose levels and glucose variability. The research highlights the importance of considering not just the quantity but also the quality of macronutrients (carbohydrates, lipids, and proteins) in managing and understanding glycemic control and cardiovascular disease risk, see [Wheeler et al. \(2012\)](#) for a review on this topic. Thus, we aimed to investigate the effect of diet composition on glucose average levels and glucose variability in subjects with and without diabetes.

The participants were a subset of those enrolled in the A Estrada Glycation and Inflammation Study (AEGIS), trial NCT01796184 at www.clinicaltrials.gov. Our analysis was performed over the $n = 509$ non-diabetic patients. For six consecutive days, the participants were asked to record their diet at the time that their food and beverages were consumed. Energy intake, macronutrients (protein, carbohydrates and lipids) and micronutrients were calculated for each meal (breakfast, lunch and dinner); more details can be found in [Gude et al. \(2017\)](#).

For each participant, the response Y corresponds to a glycaemic index that was computed as the area under the curve of glycaemic excursions during the same period, see [Service \(2013\)](#) for more details. We performed the analysis with the following compositional covariates: proteins (P), lipids (L) and carbohydrates (C) percentages ingested in a week. The assumed nonparametric model is an homoscedastic one, i.e., $Y = m(\mathbf{X}) + \sigma\epsilon$, where $\mathbf{X} = (P, L, C)^\top$ and the errors ϵ are assumed to be independent of the covariates and have distribution symmetric around 0.

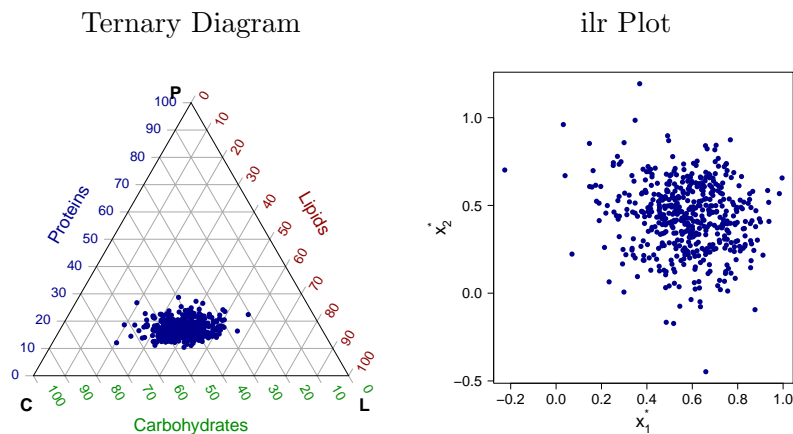


Figure 11: Ternary and ilr representations for the nutrition data.

We choose as axis in the ilr representation given by $\mathbf{x}^* = ilr(\mathbf{x}) = (x_1^*, x_2^*)^\top$, those defined as

$$x_1^* = \sqrt{\frac{1}{2}} \log \left(\frac{P}{L} \right) \quad x_2^* = \sqrt{\frac{2}{3}} \log \left(\frac{\sqrt{P L}}{C} \right).$$

Figure 11 provides the ternary representation (left panel) together with the ilr one (right panel) for the considered data set.

The nonparametric regression estimators were computed using the same loss functions as in the simulation study, that is, for the classical estimator we use the squared loss function and for the robust ones, the scale parameter was obtained using the Tukey's bisquare function with tuning constants $c_0 = 1.54764$ and $b = 1/2$, while the local M -smoother was computed using the Tukey's bisquare function with tuning constant $c_1 = 4.685$. Based on the simulation results we considered the local linear estimators.

For the analysis, we evaluate the local linear estimators at a grid of points, equally spaced in the ilr-space which was then transformed to obtain a grid of compositional points. The grid range in the ilr-space equals $[0, 1] \times [-0.3, 1]$ and has been chosen adapted to the irl-space data range and the considered grid points are displayed in yellow in Figure 12 together with the data, in the ternary plot and the irl-space. It is worth mentioning that the data points in the ilr-space show a quite spherical shape, suggesting that the ilr-components may be independent and with the same dispersion.

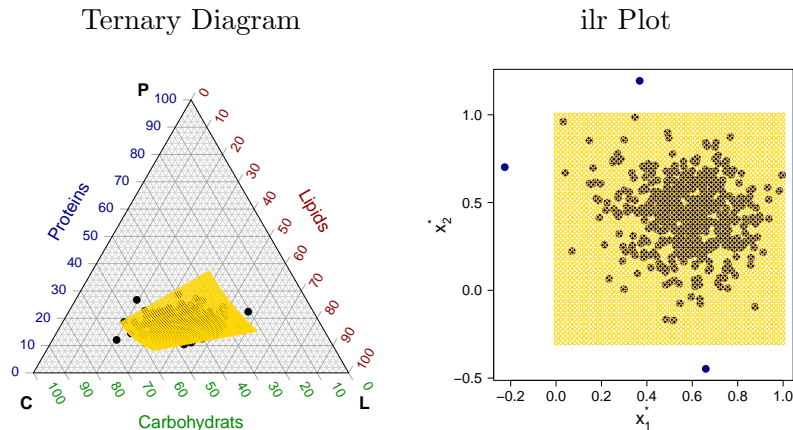


Figure 12: Grid points (in yellow) displayed on the ternary and ilr representations together with the data points. The left panel corresponds to the ternary diagram and the right one to the transformed data.

The estimators were computed using as bandwidth matrix $\mathbf{H} = h\mathbf{I}_2$, where the parameter h was selected using the robust K -fold cross-validation procedure, as described in Section 3.4, with $K = 5$ for the local linear M -smoother. For the classical estimators based on the squared loss function defined in Di Marzio et al. (2015), L^2 - K -fold cross-validation was considered. The set of candidates \mathcal{H} for the bandwidth parameter corresponds to a grid between 0.1 and 1 with step 0.1. The value 1 was selected since the maximum distance between points equal 1.66 and more than 99% of the distinct pair of points have distances lower or equal than 1. The grid was then refined around the obtained optimal bandwidth choosing a grid with step 0.02 around it. The obtained bandwidths equal 0.44 for the classical procedure and 0.22 for the robust one. It is worth mentioning that the classical procedure leads to a larger bandwidth possible due to the effect of some vertical outliers.

The obtained estimators are displayed in Figure 13 in the ilr-space. The classical and robust estimators correspond to the red and blue surfaces, respectively.

The robust estimators were also computed at the observed covariates in order to detect possible atypical observations by means of the boxplot of the residuals $\hat{r}_i = y_i - \hat{m}_R(\mathbf{x}_i)$, $i = 1, \dots, n$, where \hat{m}_R stands for the robust local linear smoother. Figure 14 displays the boxplot of the residuals which shows the presence of 17 atypical observations. Table 3 reports the observation number (N_O) and the glycaemic index of the atypical observations detected. Going back to the records, it turned out that the patients whose observation number is presented in boldface in Table 3 may be classified as prediabetic according to American Diabetes Association using other characteristics such as the A1C criteria, see ADA (2020).

The classical estimators computed without these possible atypical observations are displayed in yellow in Figure 15 in the ilr-space. The classical K -fold cross-validation bandwidth equals now 0.26 which is a value closer to the one obtained by the robust cross-validation with the whole data which was 0.22. Besides, Figure 16 shows the estimators in the ternary diagram. Again, the classical and robust estimators computed with the whole data set correspond to the red and blue surfaces, respectively, while the classical estimators computed without the atypical observations are displayed in yellow in the right panel. The selected grid points is displayed in dark gray within the ternary

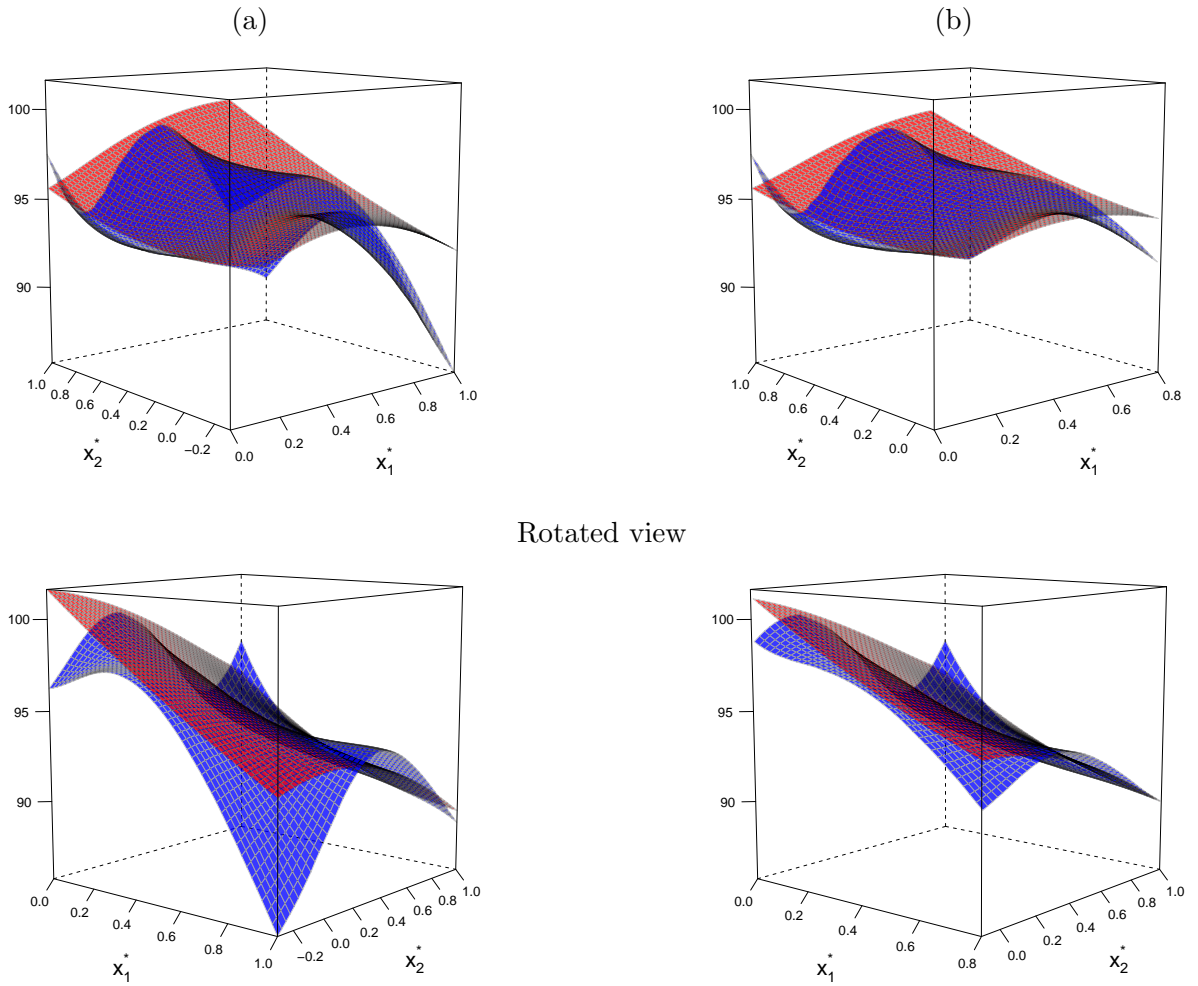


Figure 13: Predicted surfaces in the ilr -space. The plots in the left column (a) correspond to the grid range $[0, 1] \times [-0.3, 1]$, while those in (b) are displayed on the reduced range $[0, 0.8] \times [-0.1, 1]$. The classical and robust estimators correspond to the red and blue surfaces, respectively.

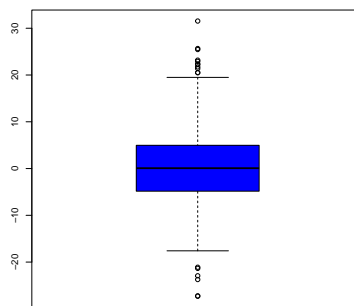


Figure 14: Boxplot of the residuals.

diagram. Note that the classical estimators computed without these potential outliers are very close to the robust ones. In other words, the robust estimator behaves similarly to the classical one if one were able to manually remove suspected outliers.

Table 3: Observation number N_O of the atypical detected observations and their corresponding glycaemic index value, y_i . Those in bold correspond to patients that were classified as pre-diabetic.

N_O	13	23	33	35	39	71	72	98	
y_i	114.69	125.60	115.20	116.35	114.54	70.36	116.62	121.58	
N_O	107	112	135	164	175	245	357	413	478
y_i	68.10	117.96	115.16	73.50	66.48	72.94	116.69	72.64	117.05

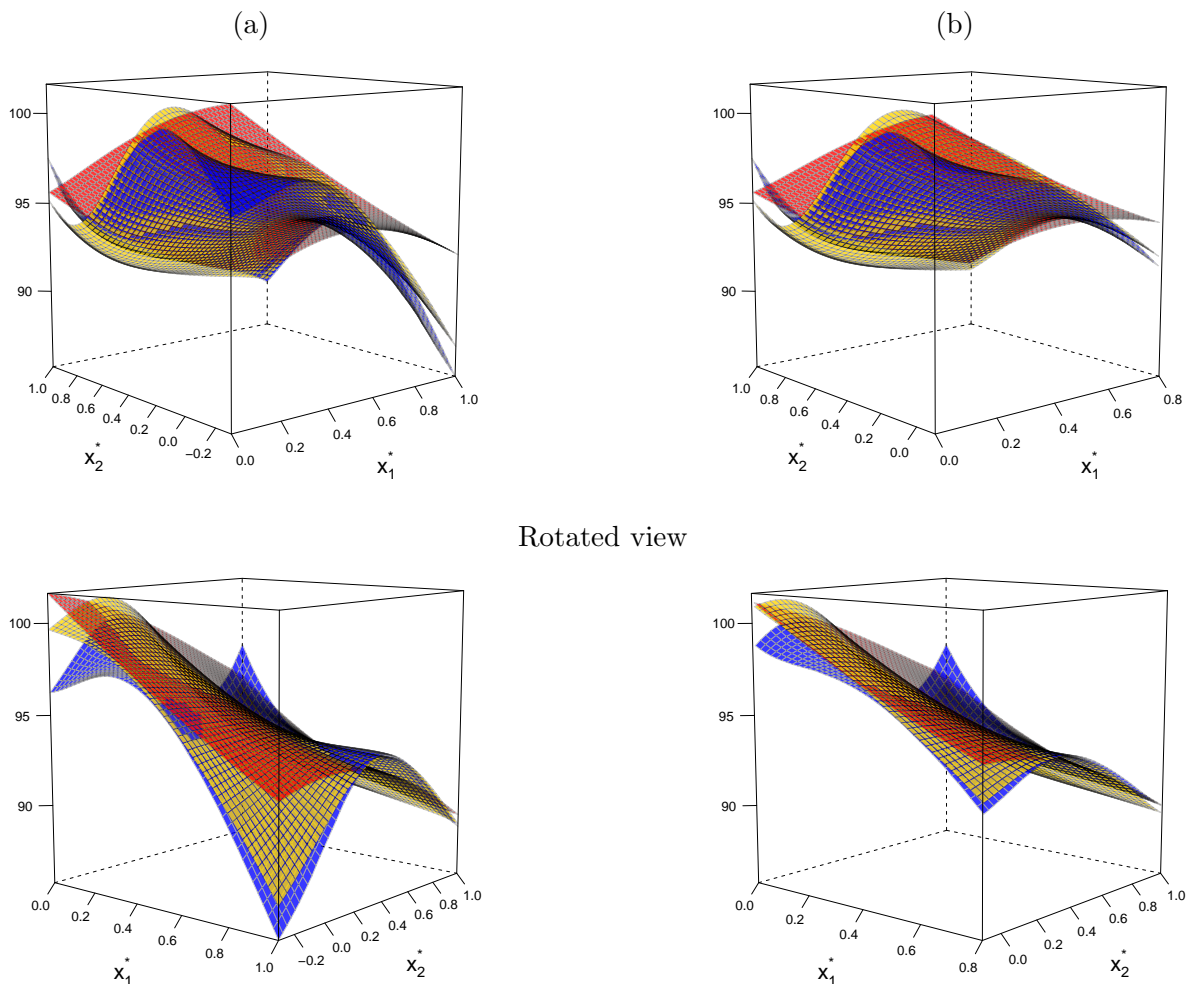


Figure 15: Predicted surfaces in the ilr-space. The plots in the left column (a) correspond to the grid range $[0, 1] \times [-0.3, 1]$, while those in (b) are displayed on the reduced range $[0, 0.8] \times [-0.1, 1]$. The classical and robust estimators computed with the whole data set correspond to the red and blue surfaces, respectively, while the classical estimators computed without the atypical observations are displayed in yellow.

Acknowledgements. This research was partially supported by Grants PICT 2021-I-A-00260 from ANPCYT and 20020170100022BA from the Universidad de Buenos Aires, Argentina and also by the Spanish Project from the Ministry of Science and Innovation (MCIU/ AEI /10.13039/501100011033) PID2020-116587GB-I00, Spain.

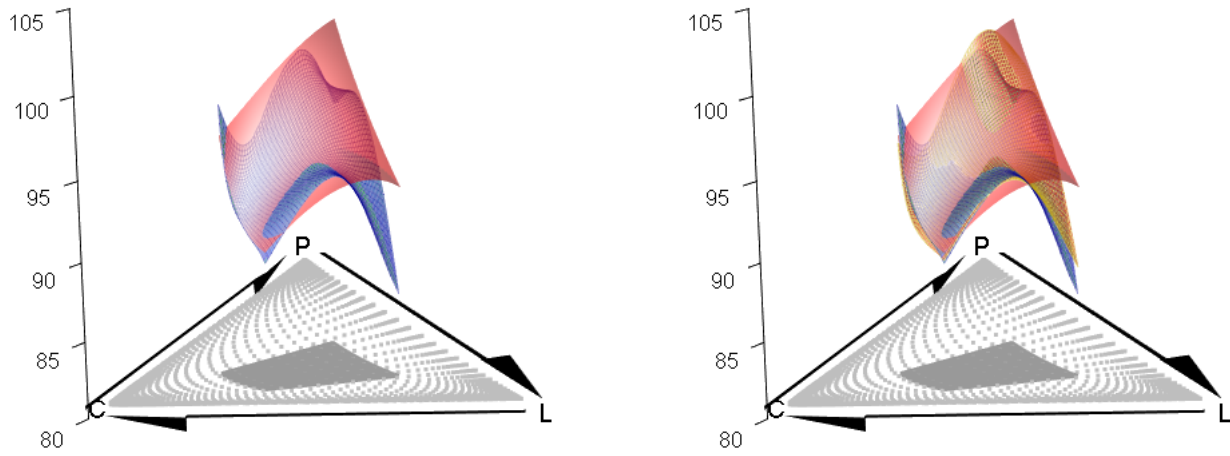


Figure 16: Predicted surfaces in the ternary diagram. The classical and robust estimators computed with the whole data set are displayed in the left panel and correspond to the red and blue surfaces, respectively. In the right panel these estimators are displayed with the classical estimators computed without the atypical observations that are displayed in yellow. The lower panel presents an animation to visualize the surfaces from different angles.

References

- ADA (2020). *2. Classification and diagnosis of diabetes: standards of medical care in diabetes-2020. Diabetes care, 43 (Supplement 1), S14-S31.* American Diabetes Association.
- Aitchison, J. (1982). The statistical analysis of compositional data. *Journal of the Royal Statistical Society. Series B (Methodological)*, 44:139–177.
- Aitchison, J. (2003). *The Statistical Analysis of Compositional Data.* The Blackburn Press.
- Aitchison, J. and Bacon-Shone, J. (1984). Log contrast models for experiments with mixtures. *Biometrika*, 71:323–330.
- Aitchison, J. and Lauder, I. J. (1985). Kernel density estimation for compositional data. *Journal of the Royal Statistical Society. Series C*, 34:129–137.
- Aitchison, J. and Shen, S. M. (1980). Logistic-normal distributions: some properties and uses. *Biometrika*, 67:261–272.
- Alenazi, A. (2021). A review of compositional data analysis and recent advances. *Communications in Statistics - Theory and Methods*, 52:5535–5567.
- Baxter, M. J., Beardah, C. C., Cool, H. E. M., and Jackson, C. M. (2005). Compositional data analysis of some alkaline glasses. *Mathematical Geology*, 37:183–196.
- Baxter, M. J. and Freestone, I. C. (2006). Log-ratio compositional data analysis in archaeometry. *Archaeometry*, 48:511–531.
- Bianco, A. and Boente, G. (2007). Robust estimators under a semiparametric partly linear autoregression model: Asymptotic behaviour and bandwidth selection. *Journal of Time Series Analysis*, 28:274–306.
- Boente, G. and Fraiman, R. (1989). Robust nonparametric regression estimation. *Journal of Multivariate Analysis*, 29:180–198.
- Boente, G., Fraiman, R., and Meloche, J. (1997). Robust nonparametric regression estimation. *Journal of Statistical Planning and Inference*, 57:109–142.
- Boente, G. and Martinez, A. (2017). Marginal integration M -estimators for additive models. *Test*, 26:231–260.
- Boente, G. and Rodriguez, D. (2008). Robust bandwidth selection in semiparametric partly linear regression models: Monte Carlo study and influential analysis. *Computational Statistics and Data Analysis*, 52:383–397.
- Cantoni, E. and Ronchetti, E. (2001). Resistant selection of the smoothing parameter for smoothing splines. *Statistics and Computing*, 11:141–146.
- Chacón, J. E., Mateu-Figueras, G., and Martín-Fernández, J. A. (2011). Gaussian kernels for density estimation with compositional data. *Computers and Geosciences*, 37:702–711.
- Cleveland, W. (1979). Robust locally weighted regression and smoothing scatterplots. *Journal of the American Statistical Association*, 74:829–836.
- Coenders, G. and Pawlowsky-Glahn, V. (2020). On interpretations of tests and effect sizes in regression models with a compositional predictor. *SORT. Statistics and Operations Research Transactions*, 44:201–220.

- Connor, R. J. and Mosimann, J. E. (1969). Concepts of independence for proportions with a generalization of the dirichlet distribution. *Journal of the American Statistical Association*, 64:194–206.
- Di Marzio, M., Panzera, A., and Venieri, C. (2015). Non-parametric regression for compositional data. *Statistical Modelling*, 15:113–133.
- Egozcue, J. J., Daunis-I-Estadella, J., Pawlowsky-Glahn, V., Hron, K., and Filzmoser, P. (2012). Simplicial regression: the normal model. *Journal of Applied Probability and Statistics*, 6:87–108.
- Egozcue, J. J., Pawlowsky-Glahn, V., Mateu-Figueras, G., and Barceló-Vidal, C. (2003). Isometric logratio transformations for compositional data analysis. *Mathematical Geology*, 35:279–300.
- Greenacre, M. (2021). Compositional data analysis. *Annual Review of Statistics and Its Application*, 8:271–299.
- Gude, F., Díaz-Vidal, P., Rúa-Pérez, C., Alonso-Sampedro, M., Fernández-Merino, C., Rey-García, J., Cadarso-Suárez, C., Pazos-Couselo, M., García-López, J. M., and Gonzalez-Quintela, A. (2017). Glycemic variability and its association with demographics and lifestyles in a general adult population. *Journal of Diabetes Science and Technology*, 11 (4):780–790.
- Härdle, W. and Tsybakov, A. B. (1988). Robust nonparametric regression with simultaneous scale curve estimation. *Annals of Statistics*, 16:120–135.
- Hijazi, R. H. and Jernigan, R. W. (2009). Modelling compositional data using dirichlet regression models. *Journal of Applied Probability and Statistics*, 4:77–91.
- Hubert, M. and Vandervieren, E. (2008). An adjusted boxplot for skewed distributions. *Computational Statistics and Data Analysis*, 52:5186–5201.
- Jiang, J. and Mack, Y. (2001). Robust local polynomial regression for dependent data. *Statistica Sinica*, 11:705–722.
- Leung, D. (2005). Cross-validation in nonparametric regression with outliers. *Annals of Statistics*, 33:2291–2310.
- Leung, D., Marriott, F., and Wu, E. (1993). Bandwidth selection in robust smoothing. *Journal of Nonparametric Statistics*, 4:333–339.
- Maronna, R., Martin, D., Yohai, V., and Salibián-Barrera, M. (2019). *Robust Statistics: Theory and Methods (with R)*. John Wiley and Sons.
- Mateu-Figueras, G. and Pawlowsky-Glahn, V. (2008). A critical approach to probability laws in geochemistry. *Mathematical Geosciences*, 40:489–502.
- Pawlowsky-Glahn, V. and Buccianti, A. (2011). *Compositional Data Analysis*. Wiley.
- Pawlowsky-Glahn, V., Egozcue, J. J., and Tolosana-Delgado, R. (2015). *Modeling and Analysis of Compositional Data*.
- Pearson, K. (1897). Mathematical contributions to the theory of evolution. on a form of spurious correlation which may arise when indices are used in the measurement of organs. *Proceedings of the Royal Society of London*, 60:489–498.
- Scheffé, H. (1958). Experiments with mixtures. *Journal of the Royal Statistical Society: Series B (Methodological)*, 20:344–360.
- Scheffé, H. (1963). The simplex-centroid design for experiments with mixtures. *Journal of the Royal Statistical Society: Series B (Methodological)*, 25:235–251.

- Service, F. J. (2013). Glucose variability. *Diabetes*, 62(5):1398–1404.
- Tsagris, M., Alenazi, A., and Stewart, C. (2023). Flexible non-parametric regression models for compositional response data with zeros. *Statistics and Computing*, 33:1–17.
- Tsagris, M. and Stewart, C. (2018). A dirichlet regression model for compositional data with zeros. *Lobachevskii Journal of Mathematics*, 39:398–412.
- Van den Boogaart, K. G., Filzmoser, P., Hron, K., Templ, M., and Tolosana-Delgado, R. (2020). Classical and robust regression analysis with compositional data. *Mathematical Geosciences*, 53:823–858.
- Wang, F. and Scott, D. (1994). The l_1 method for robust nonparametric regression. *Journal of the American Statistical Association*, 89:65–76.
- Wheeler, M. L., Dunbar, S. A., Jaacks, L. M., Karmally, W., Mayer-Davis, E. J., Wylie-Rosett, J., and Yancy, W. S. (2012). Macronutrients, food groups and eating patterns in the management of diabetes: a systematic review of the literature, 2010. *Diabetes Care*, 35 (2):434–445.